

# Differential phosphorylation signals control endocytosis of GPR15

Yukari Okamoto and Sojin Shikano\*

Department of Biochemistry and Molecular Genetics, University of Illinois at Chicago, Chicago, IL 60607-7170

**ABSTRACT** GPR15 is an orphan G protein-coupled receptor (GPCR) that serves for an HIV coreceptor and was also recently found as a novel homing receptor for T-cells implicated in colitis. We show that GPR15 undergoes a constitutive endocytosis in the absence of ligand. The endocytosis was clathrin dependent and partially dependent on  $\beta$ -arrestin in HEK293 cells, and nearly half of the internalized GPR15 receptors were recycled to the plasma membrane. An Ala mutation of the distal C-terminal Arg-354 or Ser-357, which forms a consensus phosphorylation site for basophilic kinases, markedly reduced the endocytosis, whereas phosphomimetic mutation of Ser-357 to Asp did not. Ser-357 was phosphorylated *in vitro* by multiple kinases, including PKA and PKC, and pharmacological activation of these kinases enhanced both phosphorylation of Ser-357 and endocytosis of GPR15. These results suggested that Ser-357 phosphorylation critically controls the ligand-independent endocytosis of GPR15. The functional role of Ser-357 in endocytosis was distinct from that of a conserved Ser/Thr cluster in the more proximal C-terminus, which was responsible for the  $\beta$ -arrestin- and GPCR kinase-dependent endocytosis of GPR15. Thus phosphorylation signals may differentially control cell surface density of GPR15 through endocytosis.

## Monitoring Editor

Jean E. Gruenberg  
University of Geneva

Received: Sep 2, 2016

Revised: Jun 5, 2017

Accepted: Jun 7, 2017

## INTRODUCTION

GPR15 is an orphan G protein-coupled receptor (GPCR) that serves as a coreceptor for HIV and simian immunodeficiency virus (SIV; Deng *et al.*, 1997; Vodros *et al.*, 2003; Blaak *et al.*, 2005; Riddick *et al.*, 2015) and also appears to be involved in HIV/SIV enteropathy (Maresca *et al.*, 2003; Li *et al.*, 2008). This receptor has recently received much attention for its emerging role in the T-cell homing to colon. GPR15 was found to be important for recruitment of T<sub>H</sub>17 and T<sub>H</sub>1 effector cells, as well as regulatory T (Treg) cells, to the colon in mouse colitis models, and its predominant expression in the human effector T<sub>H</sub>2 cells implied a pathogenic role of GPR15 in ulcerative colitis in human (Kim *et al.*, 2013; Bilsborough and Viney, 2015; Nguyen *et al.*, 2015; Habtezion *et al.*, 2016). GPR15 was also found to mediate homing of dendritic epidermal T-cells to skin in

fetal mice, possibly contributing to the establishment of skin barrier function (Lahl *et al.*, 2014). In addition, a more recent study revealed an anti-inflammatory function of GPR15 in vascular endothelial cells (Pan *et al.*, 2017). Collectively these findings highlight GPR15 as a novel therapeutic target of immune disorders and infectious diseases.

Because cell surface density of GPCRs dictates the magnitude of G protein signaling, elucidation of mechanisms that control cell surface expression of GPR15 will provide an important basis for developing GPR15-targeting therapeutics. We previously reported that the cell surface expression of GPR15 is promoted by a phosphorylation-dependent binding of 14-3-3 proteins to the receptor C-terminus (Chung *et al.*, 2009; Okamoto and Shikano, 2011). The 14-3-3 protein binding to the phosphorylated penultimate Ser-359 residue likely results in masking of the adjacent Arg-X-Arg-type endoplasmic reticulum retrieval signal and promotes forward trafficking of the receptor to the plasma membrane. In addition to the forward trafficking of *de novo*-synthesized receptors, the internalization of receptors from plasma membrane is another key mechanism that controls the receptor density on cell surface. It is well established that the conformational change of GPCRs induced by ligand binding facilitates the receptor phosphorylation by GPCR kinases (GRKs) and subsequent recruitment of arrestins (Lohse and Hoffmann, 2014). This leads to the displacement of G proteins from the receptor and also induces receptor internalization by

This article was published online ahead of print in MBoC in Press (<http://www.molbiolcell.org/cgi/doi/10.1091/mbc.E16-09-0627>) on June 14, 2017.

\*Address correspondence to: Sojin Shikano ([sshikano@uic.edu](mailto:sshikano@uic.edu)).

Abbreviations used: AF488, Alexa Fluor 488; FCM, flow cytometry; GPCR, G protein-coupled receptor; WT, wild type.

© 2017 Okamoto and Shikano. This article is distributed by The American Society for Cell Biology under license from the author(s). Two months after publication it is available to the public under an Attribution-Noncommercial-Share Alike 3.0 Unported Creative Commons License (<http://creativecommons.org/licenses/by-nc-sa/3.0>).

"ASCB®," "The American Society for Cell Biology®," and "Molecular Biology of the Cell®" are registered trademarks of The American Society for Cell Biology.

promoting the interaction with the endocytic coat protein clathrin (Tobin, 2008). In most cases, the internalized receptors undergo dephosphorylation and will be recycled to the plasma membrane, reestablishing the normal receptor responsiveness. In addition, recent studies revealed G protein signaling from the internalized receptors on endosomes (Vilardaga *et al.*, 2014). Thus ligand-induced endocytosis modulates the magnitude and duration of intracellular signaling by GPCRs. On the other hand, GPCRs can also undergo endocytosis constitutively in the absence of ligand (von Zastrow and Kobilka, 1994; Segredo *et al.*, 1997; Paing *et al.*, 2002; Marion *et al.*, 2004; Scarselli and Donaldson, 2009). Although its exact physiological role is generally unclear, a constitutive receptor endocytosis has important implications for intervention in human diseases. For instance, endocytosis-mediated drug delivery, combined with specific antibodies (Abs) against receptors, offers a promising strategy for selective targeting of the cells of interest (Qian *et al.*, 2002; Muro *et al.*, 2006). However, mechanisms underlying the ligand-independent constitutive endocytosis of GPCRs have received little attention, as opposed to the extensively studied ligand-induced endocytic pathway.

One particularly interesting question is whether constitutive endocytosis uses the same molecular machineries and receptor elements as those used for the ligand-induced endocytosis. Constitutive endocytosis could be a consequence of the ligand-independent basal activation of the receptor. For instance, serotonin receptor 5HT<sub>2C</sub> isoforms undergo differential endocytosis in the absence of ligand, and the rate of endocytosis correlates with their basal receptor activities (Marion *et al.*, 2004). This constitutive endocytosis depends on GRK and  $\beta$ -arrestin, a pathway used by most of the ligand-activated GPCRs. On the other hand, an increasing number of GPCRs undergo constitutive endocytosis that does not require receptor activation. The  $\beta$ <sub>2</sub> adrenergic and M3 muscarinic receptors are constitutively endocytosed in HeLa cells in a clathrin-independent manner even in the presence of antagonists (Scarselli and Donaldson, 2009). Of note, in the presence of specific agonist, these receptors are now endocytosed more rapidly in a clathrin-dependent pathway (Scarselli and Donaldson, 2009).

The ligand-induced endocytosis of GPCRs commonly requires GRK phosphorylation of a conserved Ser/Thr (S/T cluster) within the C-terminal tail (Marchese *et al.*, 2008). However, other structural determinants in the C-terminal tail can also facilitate endocytosis by being directly recognized by the endocytic machinery (Wolfe and Trejo, 2007). For instance, constitutive internalization of protease-activated receptor-1 (PAR1) and lysophosphatidic acid receptor (LPA1) is dependent on a Tyr-based and di-Leu-based motif, respectively, that interacts directly with the clathrin adaptor AP-2 (Paing *et al.*, 2006; Urs *et al.*, 2008), suggesting that such signal motif can act independently of an S/T cluster and  $\beta$ -arrestin to mediate constitutive endocytosis of GPCRs.

In the present work, we show that GPR15 undergoes a constitutive endocytosis and plasma membrane recycling in the absence of ligand. We demonstrate a critical role of kinase phosphorylation on a distal C-terminal Ser-357 in the constitutive endocytosis of GPR15, which is distinct from the conserved S/T cluster required for the use of GRK and  $\beta$ -arrestin.

## RESULTS

### GPR15 undergoes a constitutive endocytosis in the absence of ligand

We first examined whether GPR15 is constitutively internalized in the absence of ligand. GPR15 shows a robust surface expression

when expressed in HEK293 cells (Figure 1A, left, green histogram). To measure the endocytosis rate, we used an Ab feeding assay combined with a surface fluorescence quenching technique (Ingle and Scales, 2014). The transfected cells were labeled for surface GPR15 with anti-GPR15 Ab and Alexa Fluor 488 (AF488)-secondary Fab and then incubated at 37°C for the indicated time periods to allow for internalization. Remaining surface fluorescence was eliminated with anti-AF488 quenching antibody. This Ab normally quenched AF488 signal of surface GPR15 in transfected HEK293 cells by up to 95% (Supplemental Table S1). In this way, only the internalized GPR15 receptors that have no access to the quenching Ab can be detected by flow cytometry (FCM). Figure 1A (left) shows the overlaid histograms from representative samples at 60 min. The signals from the quenched cells were corrected for the background signals and normalized to the total GPR15 signal (surface plus internalized) obtained from the unquenched cells for each time point to determine the internalization rate (Figure 1A, right, red line). This assay revealed a steady increase of internalization at least up to 60 min, when ~35% of the Ab-bound receptors were internalized. On the other hand,  $\beta$ -2 adrenergic receptor ( $\beta$ 2AR), which is not efficiently internalized in the absence of ligand (Cao *et al.*, 1998), showed a much lower endocytosis rate of ~8% at 60 min (blue line).

For the GPCRs that have identified ligands, the signaling activities that occur in the absence of ectopically added ligands are conventionally regarded as ligand-independent and/or constitutive. In contrast, it is difficult to definitely prove the ligand independence of the activities of orphan GPCRs because the fetal bovine serum (FBS)-derived factors, as well as the serum-independent factors, such as those autocrined, could account for the receptor activities. We tested the serum starving of cells for 30 min before and during the assay and did not see a significant change of GPR15 endocytosis rate (Figure 1B). This suggested that the GPR15 endocytosis is not mediated by the putative FBS-derived ligands. In addition, GPR15 expression in HEK293 cells did not inhibit cyclic AMP production compared with the untransfected cells (Supplemental Figure S1), which implies the absence of GPR15 ligands in our cell culture, at least at the levels that would cause significant G protein signaling, assuming that GPR15 signals through G $\alpha$ 1, as has been suggested (Kim *et al.*, 2013). Thus we assume that the observed GPR15 internalization is the constitutive endocytosis that occurs in the absence of ectopically added ligands under standard culture conditions.

We attempted to verify constitutive endocytosis of GPR15 by confocal microscopy using HEK293 and HeLa cells. Here we show the results with HeLa cells because we generally observed a larger number of GPR15-positive vesicles on a single focal plane due to the cell flatness on the slide chambers, although we confirmed that the results were essentially same for both cells (data not shown for HEK293). Surface GPR15 labeled with anti-GPR15 Ab was allowed for endocytosis at 37°C and then visualized by AF488-conjugated secondary Ab after fixation and permeabilization. The early endosome marker EEA1 was also stained for colocalization with GPR15. The control vector-transfected cells stained with GPR15 Ab gave undetectable signal (Supplemental Figure S2), and in addition, the GPR15-transfected cells stained with GPR15 Ab but not followed by 37°C incubation showed no detectable colocalization with EEA1 (Supplemental Figure S3). After 7.5 min of incubation at 37°C, the majority of GPR15 signal in vesicles (~65%) were colocalized with EEA1 (Figure 1C and Table 1). Thus GPR15 is internalized in a ligand-independent manner when expressed in heterologous cells.

To see whether this endocytosis is specific to certain cell types and/or overexpression system, we also tested human lymphoblast

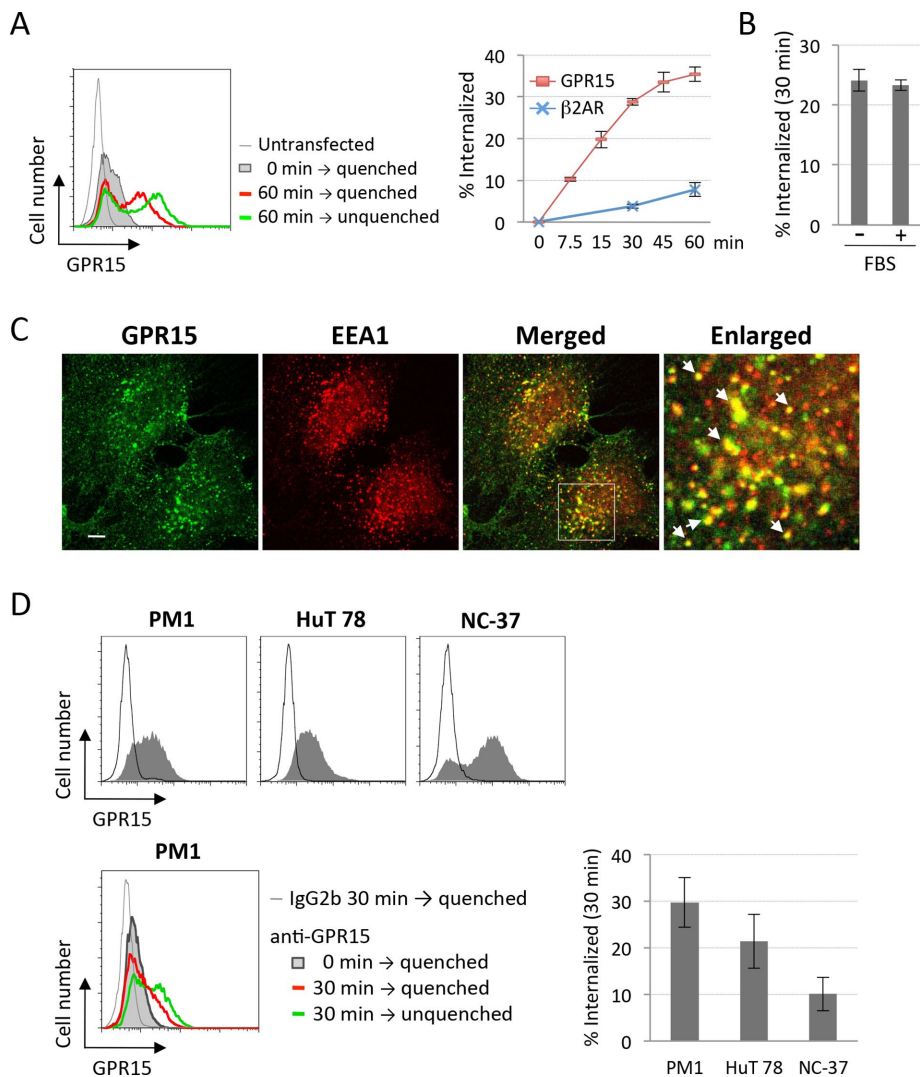


**FIGURE 1:** GPR15 undergoes a ligand-independent endocytosis. (A) Ab feeding assay of GPR15 in HEK293 cells. Left, representative histograms from FCM analysis. The quenched value after 60 min of endocytosis at 37°C (red line) was corrected for the incomplete quenching of surface fluorescence (gray filled) and normalized to the total signal (unquenched values, green line) subtracted with a background fluorescence from untransfected cells processed in parallel (light gray line) to obtain the percentage internalization. Right, internalization kinetics of WT GPR15 and  $\beta$ 2-adrenergic receptor ( $\beta$ 2AR). Internalization rate of HA-tagged  $\beta$ 2AR was determined as described for GPR15 by using AF488-anti-HA Ab. (B) Effect of FBS on GPR15 endocytosis. Cells were FBS starved or not for 30 min before and during the Ab feeding assay (30 min). (C) Localization of internalized GPR15 on endosomes. Colocalization of GPR15 (green) and EEA1 (red) was examined in HeLa cells after 7.5 min of endocytosis by confocal microscopy. The rightmost image is an enlargement of the squared region. White arrowheads indicate vesicles showing representative colocalization. Scale bar, 5  $\mu$ m. (D) Ab feeding assay of GPR15 in lymphoblast cells. Top, cell surface expression level of endogenous GPR15 as determined by anti-GPR15 Ab (gray filled) and isotype mouse IgG<sub>2b</sub> (open). Bottom left, representative histograms from Ab feeding assay with PM1 cells. Percentage internalization was determined as described in A except that background signal was measured by staining with isotype IgG<sub>2b</sub> (gray line), and the 37°C incubation was performed in the presence of fluorescence-prelabeled anti-GPR15 Ab. Bottom right, internalization rates of GPR15 in lymphoblasts at 30 min. Data are presented as mean  $\pm$  SD of three independent experiments.

cell lines that endogenously express GPR15 (Kiene et al., 2012) for constitutive endocytosis. Figure 1D, top, shows surface expression of GPR15 in T-cell lines (PM1 and Hut 78) and a B-cell line (NC-37). These cells were subjected to the Ab feeding assay for 30 min (Figure 1D, bottom left). The results demonstrated that endogenous

to the early endosomes as well (van der Sluijs et al., 1992), these data support the notion that GPR15 enters recycling pathways after ligand-independent endocytosis. We also observed partial colocalization of GPR15 with a *trans*-Golgi network (TGN) marker protein, TGN46, at 30 min (Figure 2B, bottom, and Table 1). This might also

GPR15 is also internalized constitutively in lymphoblasts at different rates, ranging from ~10 to 30% (Figure 1D, bottom right).

### Endocytosed GPR15 is recycled to the plasma membrane

Many GPCRs enter recycling compartments after internalization and return to the plasma membrane, whereas some are targeted to lysosomes for degradation. To test whether the internalized GPR15 recycles to plasma membrane, we again used an Ab-based surface fluorescence quenching technique. Transfected cells were incubated with GPR15 Ab pre-conjugated with AF488-secondary Fab at 37°C for 30 min to allow for labeling and endocytosis of GPR15. After the signal remaining on the cell surface was quenched at 4°C, the cells were shifted to 37°C for recycling in the continuous presence of quenching Ab in the medium. In this way, the recycling of the internalized GPR15 receptor will result in a decrease of fluorescence signal. To see whether the decrease of signal is truly caused by the quenching of the recycled receptor, we also did 37°C incubation after surface quenching in the absence of quenching Ab. We also performed this assay with transferrin receptor (TfR) as a positive control using AF488-conjugated transferrin. Figure 2A shows the time-course change of the remaining fluorescence signal during recycling. TfR showed nearly 90% loss of fluorescence signal within 30 min (blue), indicating efficient recycling, as reported (Padron et al., 2006). About 60% of wild-type (WT) GPR15 signal was lost in 90 min (red), whereas the no-quenching Ab control showed an ~15% decrease (green), which might represent signal loss due to receptor degradation. Thus at least ~45% of the endocytosed GPR15 is recycled to the plasma membrane within 90 min after being internalized.

To further investigate the recycling, we examined colocalization of the internalized GPR15 with Rab4 and Rab11, markers for the fast and slow recycling endosomes, respectively (Grant and Donaldson, 2009). At 7.5 min after shifting to 37°C, ~80% of the internalized GPR15 signals were colocalized with Rab4-positive endosomes (Figure 2B, top, and Table 1). GPR15 was also colocalized with Rab11 at 30 min (Figure 2B, middle, and Table 1). Although Rab4-positive vesicles may not always represent recycling endosomes because Rab4 is recruited

Marker	Percentage colocalized GPR15
EEA1	65.5 ± 2.0
Rab4	80.0 ± 6.0
Rab11	46.2 ± 12.4
TGN46	35.2 ± 17.2
Rab7	43.4 ± 5.6
LAMP1	2.4 ± 1.2
LAMP1 (+ inhibitor) <sup>a</sup>	4.4 ± 2.6

Confocal microscopy images obtained by immunocytochemistry described in Figures 2 and 3 were subjected to spot-counting analysis to determine the percentage of total GPR15-positive vesicles colocalized with the indicated marker proteins. Values are mean ± SD from 7–10 cells, which had 400–900 GPR15-positive vesicles in total.

<sup>a</sup>Endocytosis was performed in the presence of protease inhibitors E64d and pepstatin A.

**TABLE 1:** Colocalization of GPR15 with membrane markers after endocytosis.

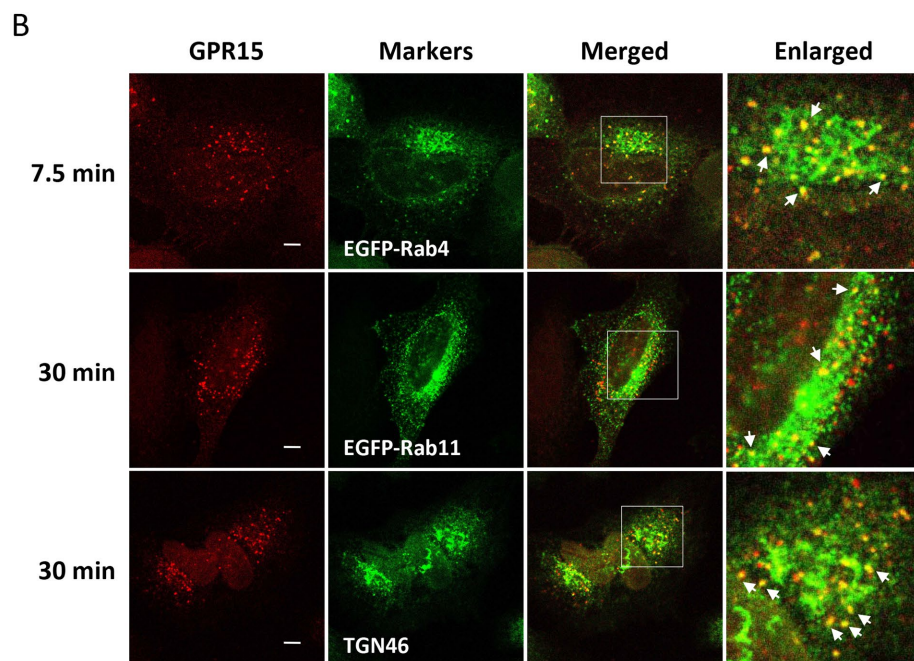
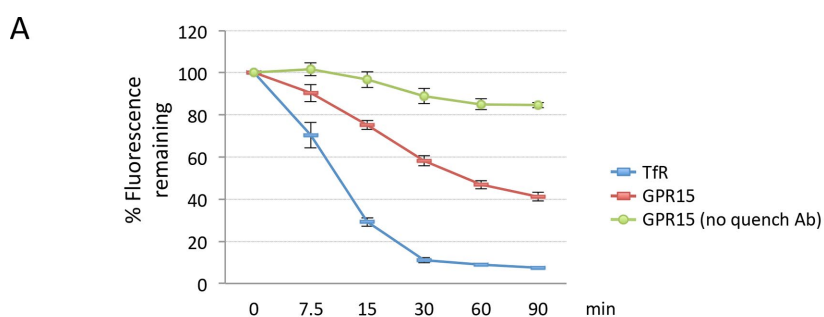


**FIGURE 2:** Endocytosed GPR15 is recycled to the plasma membrane. (A) Plasma membrane recycling assay. After the GPR15-transfected cells were incubated at 37°C for 30 min with anti-GPR15 Ab pre-conjugated with AF488-Fab, the remaining surface signal was quenched by anti-AF488 Ab at 4°C and the cells were further incubated at 37°C in the presence (red) or absence (green) of quenching Ab in the medium. Recycling of a transferrin receptor (TfR) was also measured in the same assay using HEK293 cells loaded with AF488-conjugated transferrin (blue). The remaining fluorescence from cells at each time point was measured by FCM and plotted as the percentage of prerecycling samples. (B) Intracellular localization of internalized

support recycling of GPR15 because recent studies revealed that GPCRs can retrogradely traffic from endosomes to the TGN before recycling to the plasma membrane (Csaba *et al.*, 2007; Escola *et al.*, 2010; Cheng and Filardo, 2012).

We also found that some GPR15 signals are colocalized with Rab7, a late endosome marker, at 15 min (Figure 3A and Table 1). To check whether only the Abs that might have dissociated from GPR15 receptors during the endosomal trafficking but not the receptor itself reached the Rab7 late endosome, we also used C-terminal enhanced green fluorescent protein–tagged GPR15 (GPR15-EGFP) and did observe receptor colocalization with mCherry-tagged Rab7 (Figure 3B). Because Rab7 is classically known to regulate cargo trafficking between late endosomes and lysosomes (Vitelli *et al.*, 1997; Bucci *et al.*, 2000), we examined whether the internalized GPR15 is further targeted to the lysosome by testing colocalization with a lysosomal marker, LAMP1. We found a modest colocalization of GPR15 with LAMP1 at 60 min even in the presence of protease inhibitors E64d and pepstatin A (Figure 3, C and D, and Table 1). The GPR15-EGFP also showed limited colocalization with LAMP1 regardless of 120-min treatment with protease inhibitors (Figure 3, E and F). Together

these results suggest that GPR15 are not efficiently sorted to lysosomes from Rab7-positive late endosomes. One possibility might be that GPR15 is sorted to the TGN from late endosomes, because Rab7 has been also shown to control transport from late endosomes to the TGN (Rojas *et al.*, 2008; Bastin and Heximer, 2013). Further study is necessary to elucidate the post-late endosome trafficking of GPR15.

### Constitutive endocytosis of GPR15 is dependent on clathrin

Most GPCRs are internalized in a clathrin-dependent manner. We tested the clathrin dependence of GPR15 endocytosis by coexpressing dynamin-1 K44A, a GTPase-domain mutant of dynamin that blocks the formation of clathrin-coated vesicles (Damke *et al.*, 2001). Dynamin-1 K44A effectively inhibited the endocytosis of GPR15 (Figure 4A). We also used C-AP180, a C-terminal fragment of clathrin coat assembly protein 180, which blocks specifically the clathrin-mediated endocytosis in a dominant-negative manner due to lack of binding to inositol polyphosphate in the plasma

GPR15. GPR15-transfected HeLa cells were labeled with anti-GPR15 Ab at 4°C and then incubated at 37°C for the indicated times. The internalized GPR15 was visualized by secondary Ab and examined for colocalization with membrane markers by confocal microscopy. For Rab4 and Rab11, the EGFP-fused Rab4 and Rab11 were used for cotransfection with GPR15. The rightmost images are enlargements of the squared regions. White arrowheads indicate vesicles showing colocalization of GPR15 and markers. Scale bar, 5 μm.

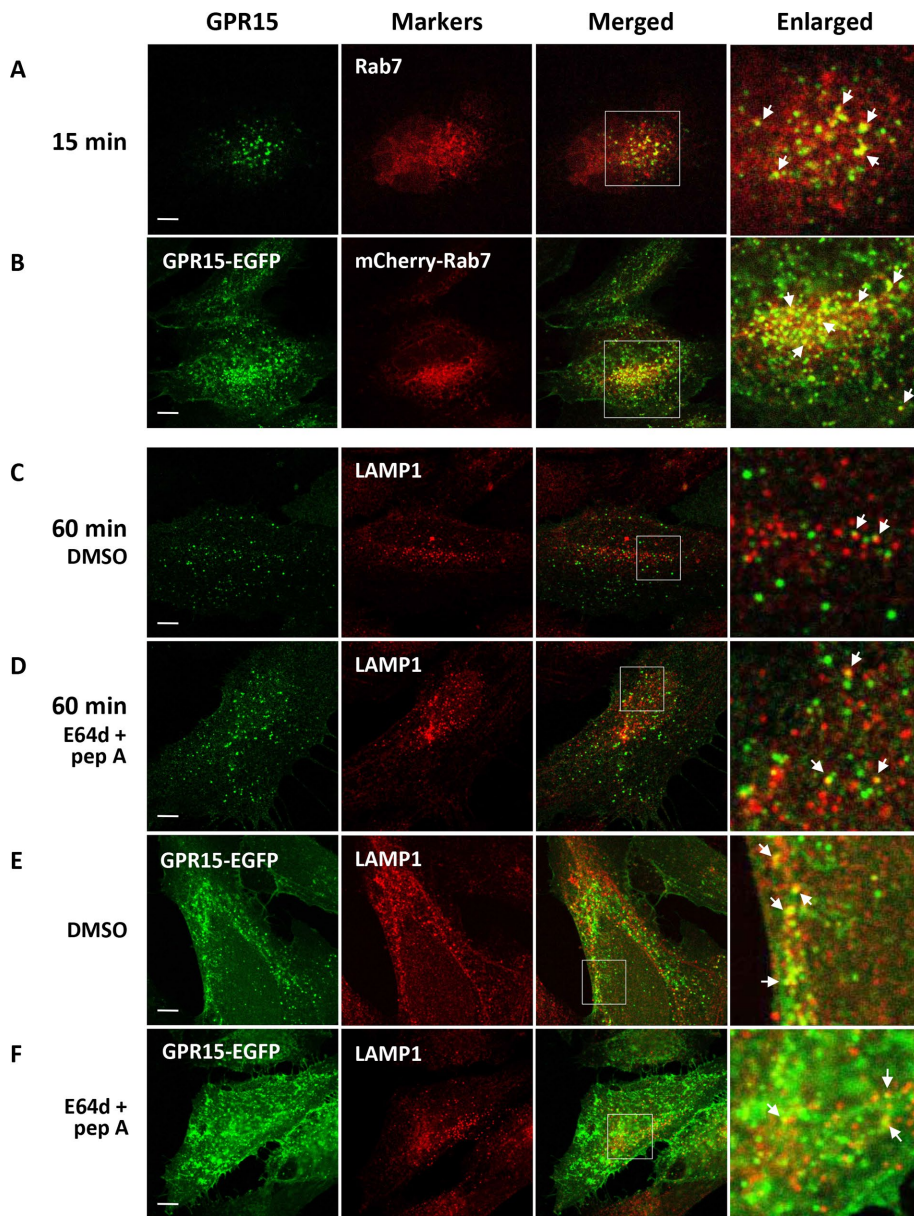


**FIGURE 3:** Endocytosed GPR15 are not efficiently sorted to lysosomes. (A) Colocalization of Ab-labeled GPR15 and Rab7 was examined at 15 min after 37°C incubation as described in Figure 2B. (B) C-terminally GFP-fused GPR15 was cotransfected with mCherry-fused Rab7 and examined for colocalization at 24 h after transfection. (C, D) Colocalization of Ab-labeled GPR15 and LAMP1 was examined at 60 min after 37°C incubation in the presence of DMSO alone or 10 μM each E64d and pepstatin A (pep A). (E, F) GPR15-GFP was examined for colocalization with LAMP1 after incubation for 2 h with DMSO alone or 10 μM each E64d and pepstatin A. The rightmost images are enlargements of the squared regions. White arrowheads indicate vesicles showing colocalization of GPR15 and markers. Scale bar, 5 μm.

membrane (Ford *et al.*, 2001). C-AP180 does not inhibit clathrin-independent endocytosis of membrane proteins (Dutta and Donaldson, 2015). The endocytosis of GPR15 was also effectively inhibited by C-AP180 (Figure 4B). These results suggest that the constitutive endocytosis of GPR15 is largely dependent on clathrin.

### Constitutive endocytosis of GPR15 requires phosphorylation of Ser-357 in the distal C-terminus

Ligand-induced endocytosis of GPCRs typically requires GRK phosphorylation of the conserved S/T cluster in the C-terminal tail

(Marchese *et al.*, 2008). GPR15 has nine Ser and Thr residues within amino acids (aa) 328–343, which correspond to this (Figure 5A). We first tested whether the S/T cluster plays a role in the constitutive endocytosis of GPR15. The Ala mutant of the S/T cluster (ST/A), which has all nine Ser and Thr residues mutated to Ala, showed a comparable endocytosis rate to that of WT GPR15 (Figure 5B), suggesting that the S/T cluster is not essential. Then we investigated other potential phosphorylation sites in the distal C-terminus (Figure 5A). Ala scanning of the C-terminal 10 residues found that the mutation in Ser-357 substantially reduced endocytosis (Figure 5C) similar to the level of dynamin-1 K44A- or C-AP180-cotransfected cells (~8%; Figure 4). The R354A mutant also showed a similar reduction of endocytosis (Figure 5C), whereas the other mutants showed no or much smaller reduction (unpublished data). We tested whether an apparently lower endocytosis rate of S357A arises from enhanced plasma membrane recycling and found that the recycling efficiency of S357A was not greater than that of WT GPR15 (Figure 5D) at any tested time points, confirming that the S357A mutation impaired the internalization step. Of importance, the Arg-354 and Ser-357 residues form a consensus phosphorylation site (R-X-X-S) for basophilic Ser/Thr kinases such as AGC-group protein kinases (Pearce *et al.*, 2010). In addition, substitution of Ser-357 with a negatively charged residue, Asp (S357D) or Glu (S357E), resulted in the internalization rates significantly higher than that of S357A mutant and similar to that of WT (Figure 5E). These data strongly suggest that phosphorylation of Ser-357, possibly mediated by AGC-group kinases, is necessary for the constitutive endocytosis of GPR15.

Next we addressed whether Ser-357 is actually phosphorylated *in vivo*. For this purpose, we sought an Ab that would specifically recognize the phosphorylated Ser-357 residue. We tested two commercial Abs from Cell Signaling Technologies, anti-phospho-protein kinase A substrate (p-PKA sub) Ab and anti-phospho-protein kinase C substrate (p-PKC sub) Ab. Note that these Abs, although referred to as PKA or PKC substrate, could potentially recognize broad sequences with phosphorylated Ser/Thr preceded by Arg or Lys residues, which are shared by AGC-group protein kinases (Pearce *et al.*, 2010). We first tested whether these Abs can detect the phosphorylation of Ser-357 by an *in vitro* binding assay using the synthetic peptides encoding GPR15 C-terminal 15 amino acids. These Abs were incubated with the agarose bead-coupled GPR15 peptides without (No-phos) or with phosphorylation on Ser-357 (p357), Ser-359 (p359), or both (p357/p359), and the bound Abs were eluted from the peptides and detected by Western blot (Figure 5F, top and middle). The p-PKA sub Ab bound

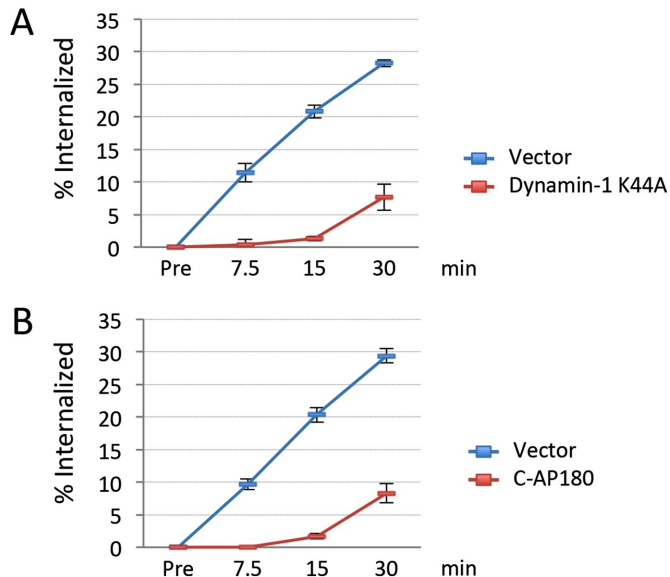


**FIGURE 4:** Constitutive endocytosis of GPR15 is dependent on clathrin. The effects of dominant-negative dynamin 1-K44A (A) and C-AP180 (B) on the constitutive endocytosis of GPR15. HEK293 cells cotransfected with GPR15 and dynamin 1-K44A, C-AP180, or control vector were examined for endocytosis by the Ab feeding assay as described for Figure 1. Data are presented as mean  $\pm$  SD of three independent experiments.

**A** ...DSYIRRAIVHCLCPCLKNYDFG SSTFTSDSHLTKALSTF IHAEDFARRRKRSVSL.

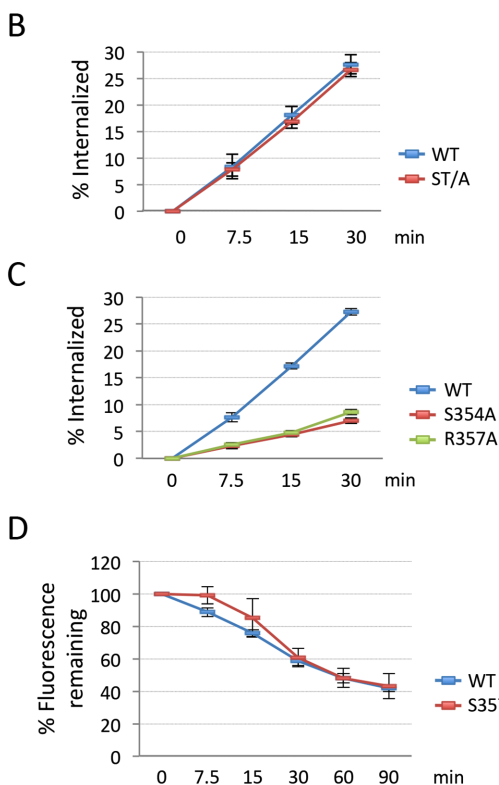
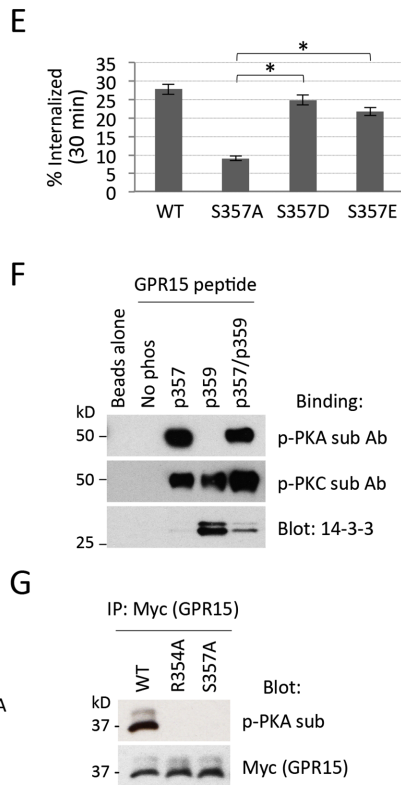


**FIGURE 5:** Constitutive endocytosis of GPR15 requires phosphorylation of Ser-357 in the distal C-terminus. (A) Sequence of GPR15 cytoplasmic tail. A conserved S/T cluster (aa 328–343) and distal Arg-354 and Ser-357 are highlighted in blue and red, respectively. (B) Internalization rates for GPR15 WT (blue) and ST/A mutant (red) were determined by the Ab feeding assay in HEK293 cells.



(C) Internalization rates for GPR15 WT (blue) and the distal C-terminal Ala mutants R354A (red) and S357A (green). (D) Plasma membrane recycling of GPR15 WT and S357A. The efficiency of plasma membrane recycling was assessed as described in Figure 2. (E) Internalization rates at 30 min for GPR15 WT, S357A, S357D, and S357E. Asterisks indicate statistically significant differences from S357A (\* $p$  < 0.01). (F) Recognition of phosphorylated Ser-357 by p-PKA sub Ab and p-PKC sub Ab. The immobilized GPR15 C-terminal peptides without (No-phos) or with phosphorylation on Ser-357 (p357), Ser-359 (p359), or both (p357/p359) were incubated with p-PKA sub Ab or p-PKC sub Ab. Top and middle, bound Abs were eluted and detected by Western blot using HRP-conjugated anti-rabbit IgG Ab. Monomeric IgG heavy chains of ~50 kDa. Bottom, peptides were further examined for the binding of 14-3-3 proteins by incubation with HEK293 cell lysate. The eluants were blotted with 14-3-3 Ab, which recognizes all seven isoforms comprising 14-3-3 $\epsilon$  (top) and the others (bottom). (G) Ser-357 phosphorylation of GPR15 in HEK293 cells. The immunoprecipitated Myc-GPR15 was probed by p-PKA sub Ab and then reprobbed by Myc Ab. The slower-migrating bands represent the O-glycosylated form. Data are presented as values  $\pm$  SD of three independent experiments.

to the p357 and p357/p359 peptides but not to the p359 peptide, whereas p-PKC sub Ab showed detectable binding to p359 as well as to p357 and p357/p359 peptides. Lack of binding of p-PKA sub Ab to p359 peptide is not due to the inefficient conjugation of this peptide to the beads, because incubation of these phosphorylated peptides with HEK293 cell lysate resulted in a robust binding of 14-3-3 proteins to p359 peptide, whereas binding to p357 peptide was minimal (Figure 5F, bottom), which is consistent with our previous finding that Ser-359 phosphorylation but not Ser-357 is necessary for 14-3-3 binding to GPR15 C-terminus (Okamoto and Shikano, 2011). Thus this commercial p-PKA sub Ab primarily recognizes phosphorylated Ser-357 rather than Ser-359. Having this, we examined whether Ser-357 residue is constitutively phosphorylated in HEK293 cells by blotting the immunoprecipitated myc-tagged GPR15 proteins with this Ab (Figure 5G). WT GPR15 protein showed strong phosphorylation signal, whereas either R354A or S357A mutation abolished the signal, indicating that this immunoblot signal for the WT GPR15 protein represents the phosphorylation of Ser-357 residue and also that Ser-357 is the only phosphorylation site within GPR15 that can be detected by this Ab. Together these data suggest that Ser-357 is constitutively phosphorylated in HEK293 cells and is necessary for ligand-independent endocytosis of GPR15.

### Kinase activation promotes Ser-357 phosphorylation and endocytosis of GPR15

As mentioned earlier, detection of Ser-357 phosphorylation by a p-PKA sub Ab (Figure 5F) does not necessarily indicate that Ser-357 is actually phosphorylated by PKA because R-X-X-S is a consensus target sequence of AGC-group protein kinases (Pearce *et al.*, 2010). We

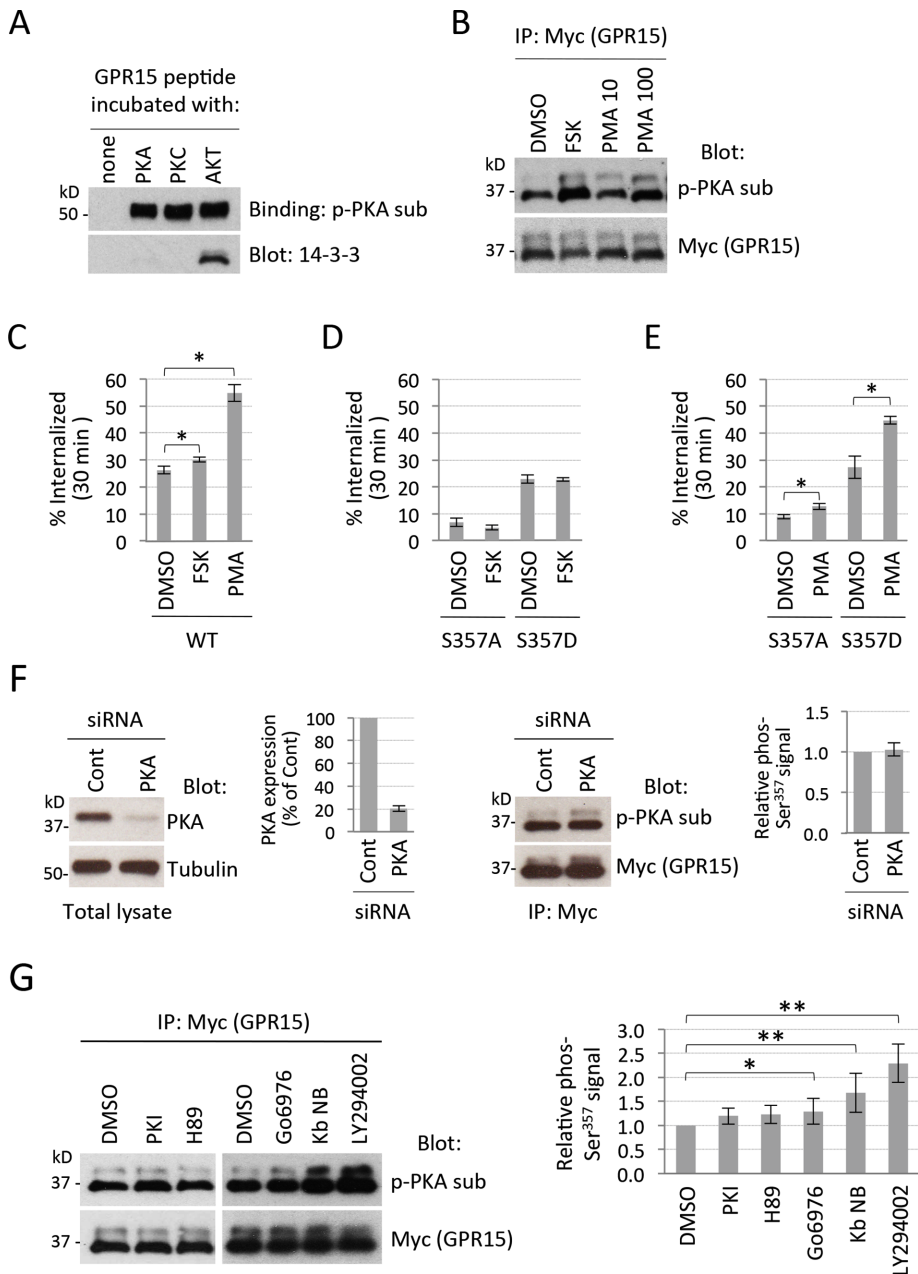


**FIGURE 6:** PKA and PKC activation promotes Ser-357 phosphorylation and endocytosis of GPR15. (A) In vitro phosphorylation of Ser-357 by basophilic kinases. Nonphosphorylated GPR15 C-terminal peptides were immobilized and incubated with the indicated recombinant kinases and then examined for Ser-357 phosphorylation by the binding of p-PKA sub Ab (top) and also for 14-3-3 binding (bottom) as described for Figure 5F. (B) In vitro effects of PKA and PKC activators on Ser-357 phosphorylation. Immunoprecipitated Myc-GPR15 from HEK293 cells treated with forskolin (FSK, 30  $\mu$ M) or PMA (10 or 100 ng/ml) for 30 min was probed with p-PKA sub Ab (top) and then re-probed with Myc Ab (bottom). (C) Effects of PKA and PKC activators on endocytosis of WT GPR15. The Ab feeding assay was performed in the presence of forskolin (FSK, 30  $\mu$ M) or PMA (10 ng/ml) for 30 min. (D, E) Effects of PKA and PKC activators on endocytosis of GPR15 Ser-357 mutants. The Ab feeding assay was performed with S357A and S357D mutants in the presence of (D) forskolin (30  $\mu$ M) or (E) PMA (10 ng/ml) for 30 min. (F) Effect of PKA knockdown on Ser-357 phosphorylation. HEK293 cells expressing Myc-GPR15 were treated with 10 nM control siRNA or siRNA against PKA catalytic subunit  $\alpha$  for 72 h. Total cell lysates were blotted for PKA catalytic subunit  $\alpha$  and  $\beta$ -tubulin (left). The immunoprecipitated Myc-GPR15 was probed with p-PKA sub Ab and then re-probed with Myc Ab (right). The band signals from p-PKA sub blot were normalized to the corresponding signals from Myc reblot. These normalized phosphorylation values are presented as the relative ratio to those from control siRNA (mean  $\pm$  SD from three experiments; right). (G) Effects of kinase inhibitors on Ser-357 phosphorylation. Cells expressing Myc-GPR15 were treated for 30 min with

tested three members of this kinase family—PKA, PKC, and AKT—for their potential to phosphorylate Ser-357 in vitro. Nonphosphorylated GPR15 C-terminal peptides were immobilized on the beads and then incubated with the purified recombinant kinases to allow for the phosphorylation. The beads were further incubated with p-PKA sub Ab, and the bound Ab was eluted and detected by Western blot. All three kinases phosphorylated the GPR15 peptide (Figure 6A, top). When these phosphorylated peptides were further incubated with HEK293 cell lysate and the eluants were immunoblotted for 14-3-3 proteins, only AKT-phosphorylated peptide showed binding of 14-3-3 (Figure 6A, bottom), although chemiluminescence with extended exposure showed very weak signal of 14-3-3 for PKA-phosphorylated peptide. Based on the requirement of Ser-359 phosphorylation for 14-3-3 binding (Okamoto and Shikano, 2011), these data suggest that PKA and PKC primarily phosphorylate Ser-357 rather than Ser-359 in vitro. On the other hand, AKT can phosphorylate Ser-357 but also Ser-359 more effectively than do PKA and PKC, which is consistent with our previous finding that PI3K/AKT activation enhances 14-3-3 binding to GPR15 (Chung et al., 2009).

Having examined the potential of PKA and PKC in specifically phosphorylating Ser-357 residue, we next addressed their in vivo role by modulating their cellular activities. Treatment with PKA activator forskolin or PKC activator phorbol 12-myristate 13-acetate (PMA) resulted in an increased phosphorylation of Ser-357, which was more apparent in the O-glycosylated form of GPR15 (slower-migrating band) that is enriched in the plasma membrane (Okamoto and Shikano, 2011; Figure 6B). These results suggest that activated PKA and PKC can phosphorylate Ser-357 in HEK293 cells. Then we tested whether these treatments also promote endocytosis of WT GPR15 by an Ab feeding assay (Figure 6C). Forskolin stimulation led to a relatively small but significant increase of the internalization rate

PKI (100  $\mu$ M), H89 (10  $\mu$ M), Go6976 (1  $\mu$ M), kb NB 142-70 (kb NB; 30  $\mu$ M), LY294002 (5  $\mu$ M), or DMSO as a vehicle control. The immunoprecipitated Myc-GPR15 was probed with p-PKA sub Ab and then re-probed with Myc Ab (left). Relative phosphorylation values were determined as described for the p-PKA sub blot in Figure 6F and presented as the relative ratio to DMSO control (mean  $\pm$  SD from three experiments; right). Asterisks indicate statistically significant differences from DMSO control (\* $p$  < 0.05, \*\* $p$  < 0.01).

(~26% for dimethyl sulfoxide [DMSO] and 30% for forskolin). In contrast, PMA treatment (10 ng/ml) markedly increased the rate to ~55%. We examined whether the effects of these activators on GPR15 endocytosis are solely attributable to the phosphorylation of Ser-357. The effect of forskolin was completely abolished when Ser-357 was mutated to Ala or Asp (Figure 6D), suggesting that forskolin indeed exerted its effect on endocytosis through phosphorylation of Ser-357. In contrast, PMA was still able to significantly enhance endocytosis of both S357A (~4%) and S357D mutants (~17%; Figure 6E). This suggested that PMA-induced endocytosis had effects on elements besides Ser-357, presumably the endocytic machinery proteins, which cannot be activated by PKA. However, it is important to note that phosphorylation of Ser-357 is still a prerequisite for PMA-induced endocytosis, because the S357A mutant showed a much smaller increase of endocytosis by PMA stimulation (Figure 6E) compared with that in WT (Figure 6C).

We also examined whether endogenous PKA activity is responsible for the constitutive phosphorylation of Ser-357 by disrupting PKA activity. Treatment with a small interfering RNA (siRNA) that reduced PKA protein expression to ~20% (Figure 6F, left) did not significantly change the basal Ser-357 phosphorylation of GPR15 (Figure 6F, right). Pharmacological inhibition of PKA by PKI and H89 also did not significantly decrease Ser-357 phosphorylation (Figure 6G). This might suggest that basal PKA activity in HEK293 cells does not contribute to the constitutive phosphorylation of Ser-357. However, disrupting one kinase activity could lead to compensatory phosphorylation by other kinases that target the same site. Indeed, treatment with PKC/PKD (PKC $\mu$ ) inhibitor Go6976, PKD inhibitor kb NB 142-70, or PI3K/AKT inhibitor LY294002 led to a significant increase of Ser-357 rather than a decrease (Figure 6G), implying redundant and compensatory activities by PKA, PKC, and AKT toward the Ser-357 residue. Thus further investigation is necessary to determine which kinases are responsible for the basal phosphorylation of Ser-357.

### Constitutive endocytosis of GPR15 is partially dependent on $\beta$ -arrestin

Because  $\beta$ -arrestin is commonly required for ligand-induced endocytosis of GPCRs, we tested whether constitutive endocytosis of GPR15 requires  $\beta$ -arrestin. GPR15 was stably expressed and examined for endocytosis in mouse embryonic fibroblast (MEF) cells from WT and  $\beta$ -arrestin-1/2 double-knockout mice ( $\beta$ -Arr1/2 KO; Figure 7A, left). The cell surface level of GPR15 was similar between these MEF cells (unpublished data).  $\beta$ -Arr1/2 KO cells appeared to show a comparable level of internalized GPR15 signal to that of WT MEF cells when examined by confocal microscopy (Figure 7A, right), indicating that GPR15 can be constitutively internalized in the absence of  $\beta$ -arrestin. Because it was technically difficult to perform our FCM-based Ab feeding assay with these MEF cells, we sought to quantitatively determine  $\beta$ -arrestin dependence by the Ab feeding assay in HEK293 cells using a dominant-negative  $\beta$ -arrestin-1 (319-418).  $\beta$ -Arr1 (319-418), a C-terminal fragment of  $\beta$ -arrestin-1, serves as a dominant-negative inhibitor for all of the  $\beta$ -arrestin isoforms by binding to clathrin and AP-2 but not to the receptors (Krupnick *et al.*, 1997). Figure 7B, left, shows the expression of transfected  $\beta$ -Arr1 (319-418), as well as of endogenous  $\beta$ -arrestin-1/2, in HEK293 cells. We first tested the specificity of the effect of  $\beta$ -Arr1 (319-418) on arrestin-dependent endocytosis by coexpressing with CXCR7 and transferrin receptor, which are known to undergo constitutive arrestin- and clathrin-dependent endocytosis (Luker *et al.*, 2010) and arrestin-independent clathrin-dependent endocytosis (Dutta and Donaldson, 2015), respectively. Coexpression of  $\beta$ -Arr1 (319-418) significantly reduced the endocytosis rate of CXCR7 from ~50 to

23% but not that of transferrin receptor (Figure 7B, right), confirming its lack of nonspecific effect on clathrin-dependent endocytosis. Under this condition, coexpression of  $\beta$ -Arr1 (319-418) with GPR15 slightly but significantly reduced the endocytosis rate at all time points (Figure 7C), suggesting that a constitutive endocytosis of GPR15 is at least partially dependent on  $\beta$ -arrestin in HEK293 cells.

### The S/T cluster but not Ser-357 is required for the GRK/ $\beta$ -arrestin-dependent endocytosis of GPR15

We were interested in the mechanistic role of Ser-357. Having found a partial  $\beta$ -arrestin dependence, we sought to determine whether Ser-357 is involved in  $\beta$ -arrestin usage by comparing it with an S/T cluster, which is one of the canonical  $\beta$ -arrestin-binding sites. Given that Figure 5B showed that the ST/A mutation did not reduce the internalization rate (also shown in Figure 8A, darker columns), we expected that the S/T cluster might not be involved in  $\beta$ -arrestin usage in the constitutive endocytosis. However, in contrast to the WT GPR15 in which  $\beta$ -Arr1 (319-418) reduced the endocytosis rate from ~30 to 23%, the ST/A mutation abolished the inhibitory effect of  $\beta$ -Arr1 (319-418) (Figure 8A, lighter columns). Our interpretation is that the S/T cluster is indeed used in arrestin-dependent endocytosis of WT GPR15 but the removal of the S/T cluster led to a receptor conformation that promoted the arrestin-independent endocytosis to confer a comparable internalization rate to that of WT GPR15. This was shown in a previous finding that the endocytosis of serotonin receptor 5HT4B is shifted from an arrestin-dependent pathway to an arrestin-independent one by the removal of the C-terminal S/T cluster without affecting the endocytosis rate itself (Barthet *et al.*, 2005). The S357A mutation was also found to abolish the sensitivity to  $\beta$ -Arr1 (319-418) (Figure 8A). This might suggest a possible involvement of Ser-357 in arrestin-dependent endocytosis. However, the already lowered endocytosis rate of S357A mutant made it difficult to evaluate precisely the effect of  $\beta$ -Arr1 (319-418). Therefore, to better address the relative roles of Ser-357 and ST cluster in  $\beta$ -arrestin usage, we decided to use a GPR15 mutant that would undergo ligand-independent endocytosis in a more  $\beta$ -arrestin-dependent manner. The Asp-Arg-Tyr (DRY) motif is a highly conserved sequence in a class A GPCRs, located at the junction of third transmembrane region and the second intracellular loop. A number of mutation studies have demonstrated that an Arg residue within this motif plays important roles in G protein coupling, receptor phosphorylation, and  $\beta$ -arrestin recruitment (Kim and Caron, 2008). In the vasopressin receptor V2R, the Arg mutation within the DRY motif (R137H) causes constitutive receptor phosphorylation and arrestin recruitment, which results in receptor desensitization and intracellular sequestration (Barak *et al.*, 2001). A previous study found that Arg mutation to Ala of a DRY motif in GPR15 inhibited the migration of GPR15-expressing Treg cells to the inflammatory site in colon (Kim *et al.*, 2013), which is consistent with a loss of G protein signaling. On this basis, we reasoned that the DAY mutant (R131A) might use a conformation with higher affinity to GRK/ $\beta$ -arrestin and therefore may serve as a model to better define the role of an S/T cluster and Ser-357 in  $\beta$ -arrestin-dependent endocytosis. As expected, our Ab feeding assay revealed significantly enhanced endocytosis by R131A mutation (Figure 8B; ~28% for WT and 50% for R131A at 30 min), similar to some of the Arg DRY mutants in other GPCRs (Barak *et al.*, 2001; Lagane *et al.*, 2005). Coexpression of the dominant-negative C-AP180 revealed a strong dependence of R131A endocytosis on clathrin, similar to that of WT GPR15 (Figure 8C). When coexpressed, the R131A mutant showed much higher sensitivity to  $\beta$ -Arr1 (319-418) than did WT GPR15 (Figure 8D; internalization rate decreased from ~30 to 23% in WT and from

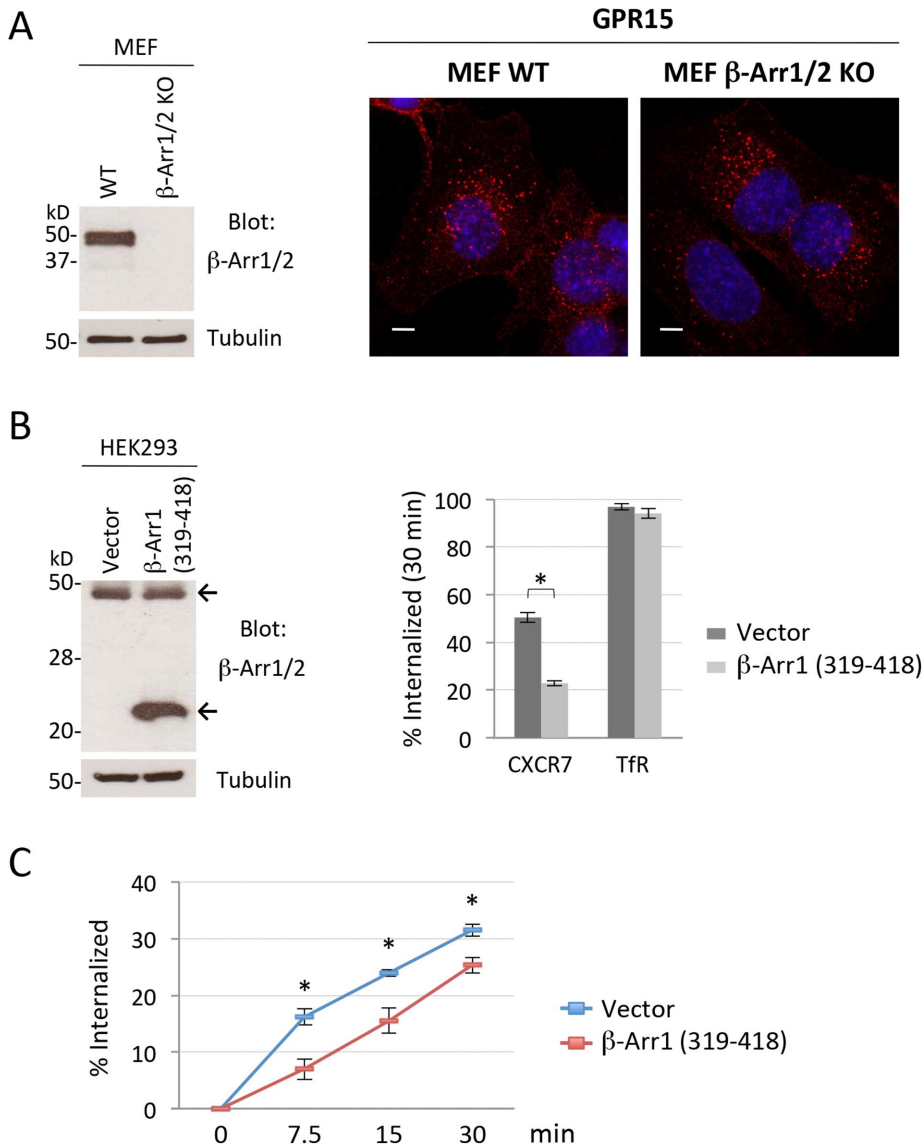


**FIGURE 7:** Constitutive endocytosis of GPR15 is partially dependent on  $\beta$ -arrestin in HEK293 cells. (A) Left, expression of endogenous  $\beta$ -arrestin-1/2 in WT and knockout MEF cells. Total lysates from WT and  $\beta$ -arrestin-1/2-knockout MEF cells were blotted with anti- $\beta$ -arrestin-1/2 Ab. Right, endocytosis of GPR15 in  $\beta$ -arrestin-1/2-knockout MEF. MEF cells transfected with GPR15 were incubated with anti-GPR15 Ab and allowed for endocytosis for 30 min at 37°C. The internalized GPR15 was labeled with a secondary Ab (red) and analyzed by confocal microscopy. Cell nuclei were counterstained with Hoechst stain (blue). (B) Left, expression of endogenous  $\beta$ -arrestin-1/2 and transfected  $\beta$ -Arr1 (319-418) in HEK293 cells. Total lysates from HEK293 cells transfected with vector or  $\beta$ -Arr1 (319-418) were blotted with anti- $\beta$ -arrestin-1/2 Ab. Upper and lower arrows indicate endogenous  $\beta$ -arrestin-1/2 and transfected  $\beta$ -Arr1 (319-418), respectively. Right, effects of  $\beta$ -Arr1 (319-418) coexpression on the endocytosis of CXCR7 and Tfr. HEK293 cells transfected with HA-CXCR7 or untransfected cells (for Tfr) were examined for the internalization rates at 30 min as described for GPR15 by using AF488-anti-HA Ab or AF488-transferrin. (C) Effect of  $\beta$ -Arr1 (319-418) coexpression on GPR15 endocytosis. The cells cotransfected with WT GPR15 and vector or  $\beta$ -Arr1 (319-418) were examined for internalization rates by the Ab feeding assay. Data are presented as mean  $\pm$  SD of three independent experiments. Asterisks indicate statistically significant differences between vector-transfected and  $\beta$ -Arr1 (319-418)-transfected cells ( $*p < 0.01$ ).

54 to 31% in R131A by  $\beta$ -Arr1 (319-418)), indicating that this mutant uses  $\beta$ -arrestin more for endocytosis than does WT. Of importance, an additional mutation in the S/T cluster of R131A significantly reduced the internalization rate (Figure 8D; ~54% for R131A and 41% for R131/ST/A at 30 min), as well as the sensitivity to  $\beta$ -Arr1 (319-418)

(internalization rate decreased from ~41 to 36% in R131/ST/A by  $\beta$ -Arr1 (319-418)). In contrast, the S357A mutation in the R131A context (R131/S357A) better preserved the sensitivity to  $\beta$ -Arr1 (319-418) (Figure 8D; internalization rate decreased from ~35 to 18% by  $\beta$ -Arr1 (319-418)) than did the R131/ST/A mutant, suggesting that the  $\beta$ -arrestin dependence of endocytosis by the R131A mutant is largely attributable to the ST cluster rather than Ser-357. The higher affinity to  $\beta$ -arrestin conceivably leads to the constitutive desensitization of the R131A mutant receptor, which may account for the lack of colon homing capacity of R131A-expressing T-cells in a mouse model (Kim *et al.*, 2013).

We also addressed the roles of Ser-357 and the S/T cluster in GRK usage by coexpressing GRKs. GRKs are Ser/Thr kinases comprising seven isoforms (GRK1–GRK7; Watari *et al.*, 2014). GRK2, GRK3, GRK5, and GRK6 are ubiquitously expressed, whereas other GRKs are expressed in limited tissues. Although GRKs had been believed to phosphorylate ligand-activated GPCRs, it is now known that they are also involved in constitutive receptor phosphorylation (Miller *et al.*, 2003; Rankin *et al.*, 2006). When coexpressed with GPR15 (Figure 8E, left), GRK2, GRK5, and GRK6 all significantly promoted the endocytosis of WT GPR15, with GRK6 being most effective (~63% internalization rate). The highest effect of GRK6 could be due to the apparently higher level of expression upon transfection (Figure 8E, right), although this awaits quantification using the same epitope-tagged GRK constructs. The promoting effects of these GRKs were not affected by S357A mutation. In contrast, ST/A mutation abolished the effects of GRK2 and GRK5 and reduced the effect of GRK6. Taken together, these results support the notion that an S/T cluster, but not Ser-357, is the primary phosphorylation site by GRKs that mediates  $\beta$ -arrestin-dependent endocytosis of GPR15. It is noteworthy that GRK6 coexpression still promoted endocytosis of the ST/A mutant, which implies additional target site(s) besides the S/T cluster in GPR15, possibly in the cytoplasmic loops (Jewell-Motz *et al.*, 2000). This is consistent with the differential phosphorylation of Ser/Thr sites by GRK isoforms (Gurevich *et al.*, 2012).

## DISCUSSION

Our quantitative Ab feeding assay revealed constitutive endocytosis of GPR15 in heterologous cells as well as in lymphoblast cells expressing the receptor endogenously. We report here that Ser-357 is constitutively phosphorylated and that this phosphorylation

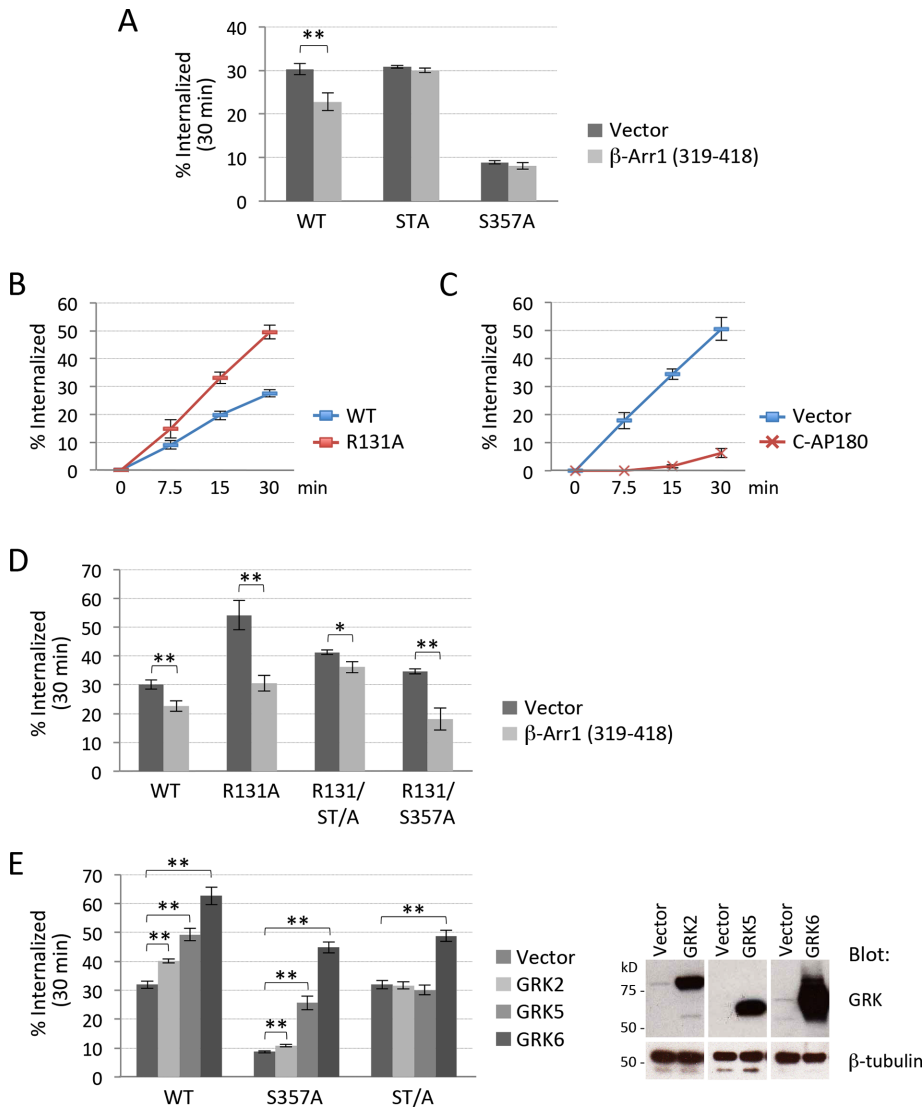


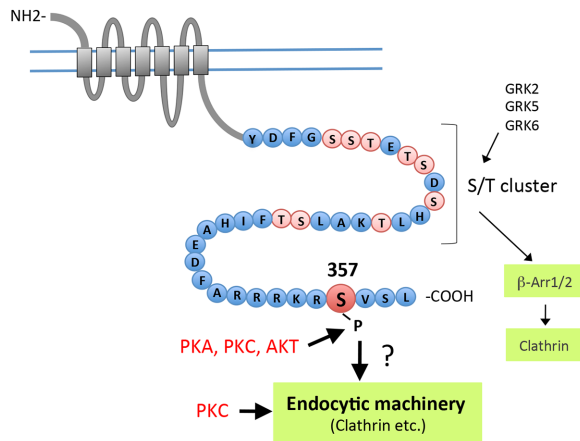
**FIGURE 8:** An S/T cluster but not Ser-357 is responsible for the GRK/ $\beta$ -arrestin-dependent endocytosis of GPR15. (A) Effect of ST/A or S357A mutation on the sensitivity to  $\beta$ -Arr1 (319-418). HEK293 cells cotransfected with GPR15 constructs and vector or  $\beta$ -Arr1 (319-418) were examined for the internalization rates at 30 min. (B) Endocytosis of GPR15 R131A mutant. The Ab feeding assay was performed with R131A mutant. (C) Clathrin dependence of R131A endocytosis. The Ab feeding assay was performed with WT and R131A mutant cotransfected with vector or C-AP180. (D) Effects of ST/A and S357A mutation in the R131A context on the sensitivity to  $\beta$ -Arr1 (319-418). HEK293 cells cotransfected with R131A mutants and vector or  $\beta$ -Arr1 (319-418) were examined for the internalization rates at 30 min. (E) Left, effects of GRK overexpression on GPR15 endocytosis. GPR15 constructs were cotransfected with vector, GRK2, GRK5, or GRK6 and measured for the internalization rates at 30 min by the Ab feeding assay. Right, expression of endogenous and transfected GRKs in HEK293 cells. GRK2, 5, and 6 in the total lysates were detected by Western blot using corresponding Abs. Data are presented as values  $\pm$  SD of three independent experiments. Asterisks indicate statistically significant differences (\* $p$  < 0.05, \*\* $p$  < 0.01).

is necessary for maximal GPR15 endocytosis. Both PKA and PKC were capable of phosphorylating Ser-357 *in vitro*, and their activation by forskolin and PMA enhanced Ser-357 phosphorylation *in vivo* (Figure 6, A and B), implicating these kinases in Ser-357 phosphorylation in HEK293 cells. An obvious question concerns how the phosphorylated Ser-357 residue would contribute to the endocytosis. We found that the GPR15 endocytosis was at least partially sensitive to a dominant-negative form of  $\beta$ -arrestin (Figure 7C). Of interest, the phosphorylation of calcium-sensing

receptor (CaR) by PKC, but not GRK2, is known to mediate  $\beta$ -arrestin binding and thereby  $\beta$ -arrestin-dependent functional desensitization (Lorenz *et al.*, 2007). In addition, PKC phosphorylation promoted internalization of the dopamine receptor D2R through a  $\beta$ -arrestin-dependent pathway (Namkung and Sibley, 2004). Thus we reasoned that Ser-357 residue, when phosphorylated, could possibly contribute to the  $\beta$ -arrestin recruitment by either creating a direct binding site or enhancing the receptor affinity to GRKs, which generally prefer to phosphorylate Ser or Thr residues in close proximity to negatively charged residues. To better define the role of Ser-357 in  $\beta$ -arrestin usage, we used a DRY motif mutant, R131A, which was constitutively internalized at a higher rate and with higher sensitivity to  $\beta$ -Arr1 (319-418) (Figure 8, B and D) than WT GPR15 and hence resembles the natural disease mutant of the DRY motif in V2R (Barak *et al.*, 2001). Conceivably, the more efficient recruitment of  $\beta$ -arrestin could account for the reported lack of migratory capacity of R131A mutant GPR15-expressing T-cells (Kim *et al.*, 2013). We found that S357A mutation in the R131A context did not affect the sensitivity to  $\beta$ -Arr1 (319-418). On the other hand, Ala mutation of an S/T cluster substantially reduced the sensitivity (Figure 8D), which suggested the primary role of an S/T cluster in  $\beta$ -arrestin usage. In addition, a markedly reduced responsiveness to GRK overexpression in ST/A but not S357A mutant (Figure 8E) further supported the notion that the S/T cluster is the primary substrate of GRKs. Taking the results together, we propose that Ser-357 phosphorylation is critically required in ligand-independent endocytosis but might play relatively less of a role when the receptor takes a conformation in which an S/T cluster is maximally used by GRKs and  $\beta$ -arrestin, presumably on binding of natural ligands to the receptor (Figure 9).

Then, would Ser-357 phosphorylation promote interaction with the endocytic machinery distinct from  $\beta$ -arrestin? Our attempt by a peptide pull-down assay to determine whether Ser-357 phosphorylation increases affinity to the clathrin adaptor AP2 failed to find such evidence (unpublished data). A GABA<sub>A</sub> receptor  $\beta$ -subunit interacts with the clathrin adaptor AP-2 through its C-terminal sequence that contains HLRRRSS, which can be phosphorylated at both Ser residues by PKA or PKC (Kittler *et al.*, 2005). Of note, this sequence is very similar to that around Ser-357 (RRRKR<sub>S</sub>) in the GPR15 C-terminus. However, in the case of GABA<sub>A</sub>, phosphorylation of these Ser residues resulted in the inhibition, as opposed to promotion, of AP-2 binding (Kittler *et al.*, 2005). On the other hand, Ser phosphorylation enhances the binding affinity of a neighboring

## Ligand (-)



## Ligand (+)

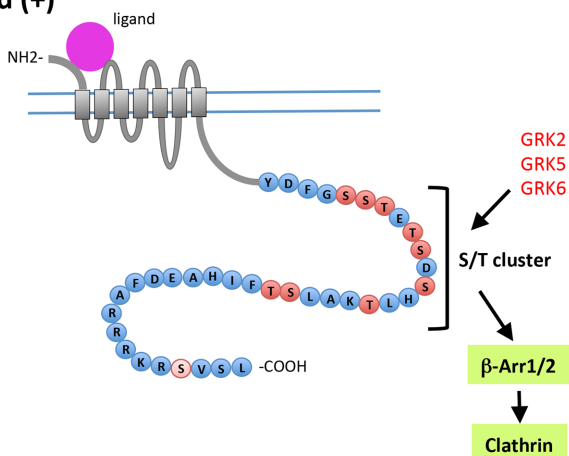


**FIGURE 9:** Working model for the relative roles of Ser-357 and S/T cluster in GPR15 endocytosis in HEK293 cells. Ser-357 is constitutively phosphorylated probably by multiple kinases, including PKA, PKC, and AKT, in a redundant manner. In the absence of ligands (top diagram), phosphorylated Ser-357 plays a primary role in promoting the clathrin-dependent endocytosis via a yet-unidentified mechanism.  $\beta$ -Arrestin partially contributes to ligand-independent endocytosis primarily via an S/T cluster phosphorylated by GRK2, 5, and 6. Activation of PKA or PKC promotes phosphorylation of Ser-357 and endocytosis of GPR15, but PKC may also act on endocytic machineries to promote endocytosis independently of Ser-357 phosphorylation. Because most GPCRs undergo  $\beta$ -arrestin-dependent endocytosis upon ligand binding, we speculate that the ligand binding to GPR15 (bottom diagram) may induce conformational change that promotes clathrin-dependent endocytosis via more efficient use of S/T cluster and  $\beta$ -arrestin, as observed with the R131A mutant.

di-Leu motif, a well-established AP-2-binding sequence, to AP-2 (Pitcher *et al.*, 1999) and promotes receptor endocytosis of CD3 $\gamma$  and CD4 (Dietrich *et al.*, 1994; Pitcher *et al.*, 1999). Thus, although there is no canonical di-Leu motif within the GPR15 C-terminus, it is possible that Ser-357 phosphorylation primes the binding of other, unidentified sequence elements to the clathrin-dependent endocytic machinery. An attempt to identify such sequence determinants is underway. It is also of interest to see whether 14-3-3 proteins that bind GPR15 (Okamoto and Shikano, 2011) play any role in endocytosis. The 14-3-3 proteins are critically involved in a wide range of cellular processes, including intracellular protein trafficking (Mackintosh, 2004; Smith *et al.*, 2011). Recent studies suggest roles for 14-3-3 in

regulating endocytosis of membrane proteins (Gabriel *et al.*, 2012; Smyth *et al.*, 2014). In the case of GPR15, however, the R356A or S359A mutation, which abolished 14-3-3 binding (Okamoto and Shikano, 2011), did not affect the endocytosis rate by our Ab feeding assay (unpublished data). Conversely, the S357A mutant, which shows poor endocytosis, retains the binding to 14-3-3 (Okamoto and Shikano, 2011). Therefore 14-3-3 binding to GPR15 is not likely involved in the constitutive endocytosis of GPR15.

Whereas stimulation with both forskolin and PMA enhanced Ser-357 phosphorylation, the promoted endocytosis of S357D by PMA (Figure 6E) indicated that the PMA effect involves kinase action toward nonreceptor elements, presumably the endocytic machinery, although Ser-357 phosphorylation is still a prerequisite, as shown by the much smaller effect of PMA in the S357A mutant (Figure 6E). On this basis, a modest effect of forskolin on endocytosis suggests that PKA cannot activate the putative endocytic machinery that is activated by PMA treatment. PMA has been shown to promote endocytosis of a number of GPCRs, as well as other surface membrane proteins (Alvi *et al.*, 2007). However, mechanistic understanding of PMA-induced endocytosis is surprisingly poor. It is conceivable that effects of PMA and the underlying mechanisms vary considerably, depending on whether the PMA-activated kinases phosphorylate the receptor itself and, if so on which sites, or act on trafficking machineries. A recent study found that PMA promotes endocytosis of  $\beta$ -arrestin-interacting GPCRs via phosphorylation of  $\beta$ -arrestin by PMA-activated ERK1/2 (Paradis *et al.*, 2015). In our case, the preserved responsiveness of the ST/A mutant to PMA treatment (unpublished data) suggests that the PMA effect on GPR15 is largely independent of  $\beta$ -arrestin and GRKs. It is tempting to speculate that PMA treatment promotes clathrin-dependent endocytosis by activating kinases such as AAK1, which associates with and phosphorylates AP-2 and enhance its affinity to the endocytosis motif on a cargo receptor (Ricotta *et al.*, 2002).

Despite many reports on the constitutive endocytosis of GPCRs (Locati *et al.*, 2005; Leterrier *et al.*, 2006; Grampp *et al.*, 2007; Scarselli and Donaldson, 2009; Lowther *et al.*, 2013), its physiological role is generally not clear. However, for some GPCRs, their constitutive endocytosis and recycling appear to be important for maintaining homeostasis. The “silent” chemokine receptor D $\delta$  suppresses inflammation by scavenging CC chemokines by constitutively shuttling between plasma membrane and endosomes (Locati *et al.*, 2005). In addition, constitutive endocytosis of type I cannabinoid receptor (CB1R) from the somatodendritic surface of neuronal cells is required for its proper axonal targeting, which contributes to the polarization of neurons (Leterrier *et al.*, 2006). Deorphanization of GPR15 will be necessary to elucidate the physiological role of its constitutive endocytosis. Nonetheless, phosphorylation-regulated endocytosis in the absence of ligand suggests that the responsiveness of GPR15-expressing cells to native ligands can be differentially controlled by other external signals by altering the steady-state surface density of the receptor.

Constitutively endocytosed receptors have been successfully used for developing a strategy to deliver therapeutic agents to target cells (Qian *et al.*, 2002; Muro *et al.*, 2006). The use of specific Abs against receptors confers specificity and efficiency to this approach by selectively targeting cells that express the receptor of interest. For instance, a broad range of therapeutic agents, including small-molecule drugs, have been conjugated with specific Ab against transferrin receptor, and their efficacy has been extensively studied (Qian *et al.*, 2002). Thus a ligand-independent endocytosis of the specific GPR15 Ab-bound receptor may provide a basis for therapeutic intervention targeting the GPR15-expressing cells such

as pathogenic T-helper cells in human ulcerative colitis (Nguyen *et al.*, 2015).

## MATERIALS AND METHODS

### Plasmids

The human GPR15 gene was cloned in pCDNA3.1(+) vector (Life Technologies), pCMVmyc vector (Okamoto and Shikano, 2011), and pEGFPN2 vector (Clontech) to generate no-tagged GPR15, N-terminal Myc-tagged GPR15, and C-terminal GFP-tagged GPR15 plasmids, respectively. CXCR4, CXCR7, and  $\beta$ 2-adrenergic receptor genes were obtained from cDNA Resource Center (Bloomsburg, PA) and cloned in pCDNA3.1(+) vector with N-terminal myc tag. K44A hemagglutinin (HA)-dynamain-1 was a gift from Sandra Schmidt (Addgene plasmid 34683). GRK2,  $\beta$ -arrestin 2 WT, and  $\beta$ -arrestin 1 (319-418) were provided by Jonathan Benovic (Thomas Jefferson University); EGFP-Rab4 and EGFP-Rab11 by Marino Zerial (Max Planck Institute), and C-AP180 by Julie Donaldson (National Institutes of Health). GRK5 and GRK6 genes were obtained from the DNASU Plasmid Repository (Tempe, AZ) and cloned in pCDNA3.1(+) vector. Site-directed mutagenesis was performed by overlap extension PCR.

### Reagents

The following reagents were used: LY294002, recombinant PKA C- $\alpha$ , and recombinant AKT1 from Cell Signaling Technology; DMSO, forskolin, PMA, chloroquine, poly-L-lysine, E64d, pepstatin A, and Go6976 from Sigma-Aldrich; Hoechst 33342 from Life Technologies; kb NB 142-70 from R&D Systems; recombinant PKC $\alpha$  from Calbiochem; and myristoylated PKI from Fisher Scientific.

### Antibodies

The following Abs were used: mouse anti-GPR15 (MAB3654) and anti-GRK5 (MAB4539) from R&D Systems; rabbit anti-GPR15 (NBP1-02651) from Novus Biologicals; mouse anti-Myc (05-724) from EMD Millipore; rabbit anti-Myc (sc-789), rabbit anti-GRK6 (sc-566), rabbit anti- $\beta$ -tubulin (sc-9104), rabbit anti-GRK2 (sc-562), rabbit anti-GRK6 (sc-566), and rabbit anti-14-3-3 $\beta$  (sc-629) from Santa Cruz Biotechnology; rabbit anti-phospho-PKA substrate (p-PKA sub, 9624), rabbit anti-phospho-PKC substrate (p-PKC sub, 2261), rabbit anti-Rab7 (9367), rabbit anti-LAMP1 (9091), rabbit anti-EEA1 (3288), rabbit anti-PKA C- $\alpha$  (5842), and rabbit anti- $\beta$ -arrestin1/2 (D24H9) from Cell Signaling Technology; sheep anti-TGN46 (AHP500GT) from AbD Serotec; AF488-mouse anti-HA (A-21287), rabbit anti-AF488 (A-11094), Cy3-goat anti-mouse immunoglobulin G (IgG; A10521), Cy3-goat anti-rabbit IgG (A10520), AF488-donkey anti-sheep IgG (A11015), AF647-goat anti-rabbit IgG (A21245), and RPE-goat anti-mouse IgG (M30004-1) from Life Technologies; horseradish peroxidase (HRP)-goat anti-rabbit IgG (PI-1000) and HRP-goat anti-mouse IgG (PI-2000) from Vector Laboratory; AF488-Fab fragment of goat anti-mouse IgG (115-547-003) and normal goat-anti mouse IgG (115-005-146) from Jackson ImmunoResearch Laboratories; AF488-streptavidin (405235) from BioLegend; normal goat serum from Thermo Fisher; and human AB serum from Sigma-Aldrich.

### Cell culture and transfection

HEK293 cells were maintained in 50% DMEM/50% Ham's F-12 medium containing 10% FBS, 2 mM L-glutamine, 100 U/ml penicillin, and 100  $\mu$ g/ml streptomycin (complete medium). HeLa cells were cultured in DMEM with the same supplements. MEF cells from WT and  $\beta$ -arrestin-1/2 double-knockout mice were obtained from Robert Lefkowitz (Duke University) and maintained in DMEM with the same supplements. PM1, HuT 78, and NC-37 cells were obtained from the NIH AIDS Reagent Program and maintained in RPMI 1640 with the

same supplements except that FBS was added at 20% for HuT 78. In some experiments, the tissue culture plates were coated with poly-L-lysine before plating cells. Transient transfection of plasmids was performed using Mirus TransIT-LT1 (Mirus Bio) according to the manufacturer's instructions. For MEF cells, expression of GPR15 was achieved by retroviral transfer of pBabe-puro vectors encoding GPR15.

### Flow cytometry

The fluorescence signal was measured with Cell Lab Quanta SC (Beckman Coulter) and analyzed using FlowJo software (Tree Star, Ashland, OR). To assure the quantitiveness of our assay, we verified that the fluorescence intensity values obtained by FCM analysis are all within the range in which the fluorescence intensities are linearly proportional to the actual numbers of fluorochromes by using Quantum MESF microspheres (Bangs Laboratories, Fishers, IN) as an external standard.

### Ab feeding assay

The internalization rate of GPR15 was determined by a fluorescence-based Ab feeding assay (Ingle and Scales, 2014) with some modifications. Briefly, HEK293 cells transiently transfected with GPR15 in six-well plates were collected by gentle pipetting at 24 h after transfection. Cells were incubated at 4°C for 20 min with mouse anti-GPR15 Ab, followed by 15 min of incubation with AF488-Fab fragment of goat anti-mouse IgG in a complete medium containing 4-(2-hydroxyethyl)-1-piperazineethanesulfonic acid (HEPES) to label cell surface GPR15. The stained cells were replated in 96-well plates in a complete medium containing HEPES and incubated at 37°C for the indicated times to allow for the receptor internalization. Then the plates were chilled on ice to stop endocytosis, and the cells were incubated with anti-AF488 quenching Ab for 30 min at 4°C to eliminate the remaining cell surface fluorescence. This Ab normally quenches up to 95% of the surface GPR15 signal expressed in HEK293 cells (Supplemental Table S1). The cells were finally fixed with 1% paraformaldehyde and analyzed for the AF488 signal by FCM. All of the fluorescence values from GPR15-transfected cells were first subtracted with the values from untransfected cells. The signal from quenching Ab-treated cells that had been incubated at 4°C (no endocytosis control) served as a background value, which represents the incomplete quenching of surface fluorescence. This background value was subtracted from the values for quenched cells that had been incubated at 37°C for each time period, which gave the net amount of internalized GPR15. These values were normalized to the total GPR15 signal (surface plus internalized) obtained from the cells processed in parallel without quenching Ab treatment at each time point to determine the internalization rate (percent). For lymphoblast cells expressing endogenous GPR15, the Ab feeding assay was performed, and percentage internalization was determined as described for GPR15-transfected HEK293 cells, except that background signal was measured by staining cells with AF488-conjugated isotype IgG<sub>2b</sub>, and the 37°C incubation was performed in the presence of anti-GPR15 Ab pre-conjugated with AF488-Fab. For endocytosis assay with HA- $\beta$ 2AR and HA-CXCR7, the AF488-labeled HA Ab was used for labeling the receptors. For transferrin receptor, GPR15-transfected HEK293 cells were incubated with AF488-conjugated transferrin for 30 min at 37°C and then processed as described for GPR15 to measure the intracellular fluorescence signal.

### Plasma membrane recycling assay

GPR15-transfected cells were incubated at 37°C for 30 min with anti-GPR15 Ab pre-conjugated with AF488-secondary Fab Ab to

allow for receptor labeling and endocytosis. The fluorescence signal remaining on the cell surface was quenched by anti-AF488 Ab in the culture medium for 30 min at 4°C and then shifted to 37°C for recycling in the continuous presence of quenching Ab. In this way, the fluorescence signal of the receptors that recycled to plasma membrane are quenched. For the no-quenching Ab control, the cells were washed after surface quenching and then incubated at 4°C with 15 µg/ml AF488-conjugated streptavidin in order to mask any unoccupied epitopes of the surface-bound quenching Ab. These cells were then shifted to 37°C for recycling in medium not containing quenching Ab. We assume that loss of fluorescence signal in the no-quenching Ab control represents the recycling-independent events, for example, receptor degradation. The fluorescence signal of cells at the indicated recycling time points was measured by FCM and is shown as the percentage of prerecycling values.

### Immunocytochemistry

HeLa cells were plated for GPR15 transfection in four-well chamber slides (Nunc) precoated with poly-L-lysine. About 24 h after transfection, cells were incubated with mouse anti-GPR15 Ab for 20 min at 4°C, washed, and then incubated at 37°C for the indicated times to allow for endocytosis in the presence or absence of drugs. The cells were fixed with Cytofix/Cytoperm buffer (BD Biosciences) for 15 min at 4°C and then permeabilized with -20°C-chilled 90% methanol for 5 min at room temperature. After blocking with 10% human AB serum, cells were stained with corresponding primary Abs to the intracellular markers overnight at 4°C. Then cells were stained with Cy3- and AF488-labeled secondary Abs at the same time for 1 h at 4°C to visualize GPR15 and marker proteins, except that TGN46 was first visualized by AF488-donkey anti-sheep Ab, blocked with 20% normal goat serum (NGS), and then stained with Cy3-goat anti-mouse Ab in 10% NGS to visualize GPR15. When EGFP-Rab4 or EGFP-Rab11 was cotransfected with GPR15, Cy3-labeled secondary Ab was used for GPR15. For the endocytosis assay with MEF cells, the cells were first labeled with anti-GPR15 Ab for 20 min at 4°C and then incubated at 37°C for 15 min to allow for endocytosis. To visualize only the internalized GPR15, the epitope of the GPR15 Ab on the surface was blocked by incubating the cells with unconjugated goat anti-mouse IgG at 4°C. After fixation and permeabilization as described, internalized GPR15 was labeled with Cy3-labeled goat anti-mouse IgG. Cells were counterstained with Hoechst 33342 (not shown) for 10 min before being mounted with Prolong Diamond mounting medium (Life Technologies). Images were collected with a Zeiss LSM 700 confocal laser scanning microscope using LSM Image Browser (Zeiss) software.

### cAMP assay

Untransfected HEK293 cells and stably GPR15-expressing HEK293 cells plated in a poly-L-lysine-coated 96-well plates were incubated with DMSO alone or with 0.5 or 1 µM forskolin in DMSO. The cells were washed with phosphate-buffered saline (PBS) and lysed, and then the lysate samples were subjected to quantitation of cAMP by the competition enzyme-linked immunoassay using the Cyclic AMP XP Chemiluminescent Assay Kit (Cell Signaling) according to the manufacturer's instruction. Relative light units (RLUs) from forskolin-treated cells are shown as percentage of those from DMSO control cells (average ± SD) in triplicate wells.

### Immunoprecipitation

HEK293 cells transfected with Myc-tagged constructs in six-well plates were washed with PBS and lysed with lysis buffer (0.5%

Igepal, 25 mM Tris, 150 mM NaCl, pH 7.5) containing protease inhibitor cocktails for 20 min at 4°C. After centrifugation for 15 min at 11,000 × *g*, the supernatant was mixed with 4 µg of mouse anti-Myc Ab and protein G-conjugated agarose beads (Life Technologies). After overnight incubation at 4°C, the beads were washed three times with lysis buffer, and then the immunoprecipitated proteins were eluted by incubating the beads with 2× Laemmli sample buffer at room temperature for 30 min.

### Phospho-PKA/PKC substrate Ab binding assay

The peptides encoding the last 15 C-terminal residues of GPR15 with or without phosphorylation on Ser-357, Ser-359, or both were synthesized by GenScript (Piscataway, NJ). The peptides were covalently coupled to Sulfo Link Coupling Resin (Thermo Scientific) through N-terminal Cys according to the manufacturer's instructions. Bead-immobilized peptides of ~10 nmol were incubated with 1 µl of p-PKA sub or p-PKC sub Ab for 1 h at 4°C. After wash, the beads were boiled with sample buffer. The peptide-bound Abs were detected by resolving eluates on SDS-PAGE followed by Western blotting using HRP-goat anti-rabbit IgG.

### In vitro phosphorylation assay

The synthetic GPR15 peptide without phosphorylation was immobilized as described and incubated for 30 min at 30°C with 100 ng of recombinant PKA, PKC, or AKT in kinase buffer (Cell Signaling Technology) supplemented with 200 µM ATP. After wash, the beads were further incubated with p-PKA sub Ab at 4°C and examined for the Ab binding by Western blot as described.

### siRNA knockdown of PKA

Cells were first transfected with 10 nM control siRNA (D-001206-13-05; GE Dharmacon) or siRNA against PKA catalytic subunit  $\alpha$  (6406S; Cell Signaling Technology) using Lipofectamine RNAiMAX (ThermoFisher). After 24 h, the cells were replated and then on the next day transfected with GPR15. The cells were lysed at 24 h after GPR15 transfection for analyses of PKA expression and GPR15 phosphorylation.

### SDS-PAGE and Western blots

The protein samples resolved on Tris-HCl polyacrylamide gels were transferred to nitrocellulose membranes and blocked with skim milk. Membranes were incubated with primary Abs for 1 h at room temperature or overnight at 4°C and then with HRP-goat anti-rabbit or anti-mouse IgG Ab. Blot signals were obtained using enhanced chemiluminescence substrate (Thermo Scientific). For reprobing of transfer membranes, the membranes were incubated in a stripping buffer (1.5% glycine, 2% SDS, pH 2.50) for 30 min at 50°C before the reblot.

### Statistical analysis

Data are presented as mean ± SD from three independent experiments. Statistical significance was assessed with a Student's *t* test between a pair of data sets. *p* < 0.05 was considered significant.

### ACKNOWLEDGMENTS

We thank Sandra Schmidt, Jonathan Benovic, Marino Zerial, and Julie Donaldson for providing plasmid vectors. We also thank Robert Lefkowitz for  $\beta$ -arrestin-1/2 knockout MEF cells. This study was supported by National Institutes of Health Grant 1R01GM099974-01 and LUNGevity Foundation/American Cancer Society Lung Cancer Research Grant 2009-07001-00-00 (to S. S.).

## REFERENCES

- Alvi F, Idkowiak-Baldys J, Baldys A, Raymond JR, Hannun YA (2007). Regulation of membrane trafficking and endocytosis by protein kinase C: emerging role of the pericentration, a novel protein kinase C-dependent subset of recycling endosomes. *Cell Mol Life Sci* 64, 263–270.
- Barak LS, Oakley RH, Laporte SA, Caron MG (2001). Constitutive arrestin-mediated desensitization of a human vasopressin receptor mutant associated with nephrogenic diabetes insipidus. *Proc Natl Acad Sci USA* 98, 93–98.
- Barthet G, Gaven F, Framery B, Shinjo K, Nakamura T, Claeysen S, Bockaert J, Dumuis A (2005). Uncoupling and endocytosis of 5-hydroxytryptamine 4 receptors. Distinct molecular events with different GRK2 requirements. *J Biol Chem* 280, 27924–27934.
- Bastin G, Heximer SP (2013). Rab family proteins regulate the endosomal trafficking and function of RGS4. *J Biol Chem* 288, 21836–21849.
- Bilsborough J, Viney JL (2015). GPR15: a tale of two species. *Nat Immunol* 16, 137–139.
- Blaak H, Boers PH, Gruters RA, Schuitemaker H, van der Ende ME, Osterhaus AD (2005). CCR5, GPR15, CXCR6 are major coreceptors of human immunodeficiency virus type 2 variants isolated from individuals with and without plasma viremia. *J Virol* 79, 1686–1700.
- Bucci C, Thomsen P, Nicoziani P, McCarthy J, van Deurs B (2000). Rab7: a key to lysosome biogenesis. *Mol Biol Cell* 11, 467–480.
- Cao TT, Mays RW, von Zastrow M (1998). Regulated endocytosis of G-protein-coupled receptors by a biochemically and functionally distinct subpopulation of clathrin-coated pits. *J Biol Chem* 273, 24592–24602.
- Cheng SB, Filardo EJ (2012). Trans-Golgi Network (TGN) as a regulatory node for beta1-adrenergic receptor (beta1AR) down-modulation and recycling. *J Biol Chem* 287, 14178–14191.
- Chung JJ, Okamoto Y, Coblitz B, Li M, Qiu Y, Shikano S (2009). PI3K/Akt signalling-mediated protein surface expression sensed by 14-3-3 interacting motif. *FEBS J* 276, 5547–5558.
- Csaba Z, Lelouvier B, Viollet C, El Ghouzi V, Toyama K, Videau C, Bernard V, Dournaud P (2007). Activated somatostatin type 2 receptors traffic in vivo in central neurons from dendrites to the trans Golgi before recycling. *Traffic* 8, 820–834.
- Damke H, Binns DD, Ueda H, Schmid SL, Baba T (2001). Dynamin GTPase domain mutants block endocytic vesicle formation at morphologically distinct stages. *Mol Biol Cell* 12, 2578–2589.
- Deng HK, Unutmaz D, KewalRamani VN, Littman DR (1997). Expression cloning of new receptors used by simian and human immunodeficiency viruses. *Nature* 388, 296–300.
- Dietrich J, Hou X, Wegener AM, Geisler C (1994). CD3 gamma contains a phosphoserine-dependent di-leucine motif involved in down-regulation of the T cell receptor. *EMBO J* 13, 2156–2166.
- Dutta D, Donaldson JG (2015). Sorting of clathrin-independent cargo proteins depends on Rab35 delivered by clathrin-mediated endocytosis. *Traffic* 16, 994–1009.
- Escola JM, Kuenzi G, Gaertner H, Foti M, Hartley O (2010). CC chemokine receptor 5 (CCR5) desensitization: cycling receptors accumulate in the trans-Golgi network. *J Biol Chem* 285, 41772–41780.
- Ford MG, Pearce BM, Higgins MK, Vallis Y, Owen DJ, Gibson A, Hopkins CR, Evans PR, McMahon HT (2001). Simultaneous binding of PtdIns(4,5)P2 and clathrin by AP180 in the nucleation of clathrin lattices on membranes. *Science* 291, 1051–1055.
- Gabriel L, Lvov A, Orthodoxou D, Rittenhouse AR, Kobertz WR, Melikian HE (2012). The acid-sensitive, anesthetic-activated potassium leak channel, KCNK3, is regulated by 14-3-3beta-dependent, protein kinase C (PKC)-mediated endocytic trafficking. *J Biol Chem* 287, 32354–32366.
- Grampp T, Sauter K, Markovic B, Benke D (2007). Gamma-aminobutyric acid type B receptors are constitutively internalized via the clathrin-dependent pathway and targeted to lysosomes for degradation. *J Biol Chem* 282, 24157–24165.
- Grant BD, Donaldson JG (2009). Pathways and mechanisms of endocytic recycling. *Nat Rev Mol Cell Biol* 10, 597–608.
- Gurevich EV, Tesmer JJ, Mushegian A, Gurevich VV (2012). G protein-coupled receptor kinases: more than just kinases and not only for GPCRs. *Pharmacol Ther* 133, 40–69.
- Habtezion A, Nguyen LP, Hadeiba H, Butcher EC (2016). Leukocyte trafficking to the small intestine and colon. *Gastroenterology* 150, 340–354.
- Ingle GS, Scales SJ (2014). DropArray, a wall-less 96-well plate for uptake and immunofluorescence microscopy, confirms CD22 recycles. *Traffic* 15, 255–272.
- Jewell-Motz EA, Small KM, Theiss CT, Liggett SB (2000). alpha 2A/alpha 2C-adrenergic receptor third loop chimera show that agonist interaction with receptor subtype backbone establishes G protein-coupled receptor kinase phosphorylation. *J Biol Chem* 275, 28989–28993.
- Kiene M, Marzi A, Urbanczyk A, Bertram S, Fisch T, Nehlmeier I, Gnirss K, Karsten CB, Palesch D, Munch J, et al. (2012). The role of the alternative coreceptor GPR15 in HIV tropism for human cells. *Virology* 433, 73–84.
- Kim KM, Caron MG (2008). Complementary roles of the DRY motif and C-terminus tail of GPCRs for G protein coupling and beta-arrestin interaction. *Biochem Biophys Res Commun* 366, 42–47.
- Kim SV, Xiang WW, Kwak C, Yang Y, Lin XW, Ota M, Sarpel U, Rifkin DB, Xu R, Littman DR (2013). GPR15-mediated homing controls immune homeostasis in the large intestine mucosa. *Science* 340, 1456–1459.
- Kittler JT, Chen G, Honing S, Bogdanov Y, McAnish K, Arancia-Carcamo IL, Jovanovic JN, Pangalos MN, Haucke V, Yan Z, Moss SJ (2005). Phospho-dependent binding of the clathrin AP2 adaptor complex to GABAA receptors regulates the efficacy of inhibitory synaptic transmission. *Proc Natl Acad Sci USA* 102, 14871–14876.
- Krupnick JG, Santini F, Gagnon AW, Keen JH, Benovic JL (1997). Modulation of the arrestin-clathrin interaction in cells. Characterization of beta-arrestin dominant-negative mutants. *J Biol Chem* 272, 32507–32512.
- Lagane B, Ballet S, Planchenault T, Balabanyan K, Le Poul E, Blanpain C, Percherancier Y, Staropoli I, Vassart G, Oppermann M, et al. (2005). Mutation of the DRY motif reveals different structural requirements for the CC chemokine receptor 5-mediated signaling and receptor endocytosis. *Mol Pharmacol* 67, 1966–1976.
- Lahl K, Sweere J, Pan J, Butcher E (2014). Orphan chemoattractant receptor GPR15 mediates dendritic epidermal T-cell recruitment to the skin. *Eur J Immunol* 44, 2577–2581.
- Leterrier C, Laine J, Darmon M, Boudin H, Rossier J, Lenkei Z (2006). Constitutive activation drives compartment-selective endocytosis and axonal targeting of type 1 cannabinoid receptors. *J Neurosci* 26, 3141–3153.
- Li Q, Estes JD, Duan L, Jessurun J, Pambuccian S, Forster C, Wietgreffe S, Zupancic M, Schacker T, Reilly C, et al. (2008). Simian immunodeficiency virus-induced intestinal cell apoptosis is the underlying mechanism of the regenerative enteropathy of early infection. *J Infect Dis* 197, 420–429.
- Locati M, Torre YM, Galliera E, Bonecchi R, Bodduluri H, Vago G, Vecchi A, Mantovani A (2005). Silent chemoattractant receptors: D6 as a decoy and scavenger receptor for inflammatory CC chemokines. *Cytokine Growth Factor Rev* 16, 679–686.
- Lohse MJ, Hoffmann C (2014). Arrestin interactions with G protein-coupled receptors. *Handb Exp Pharmacol* 219, 15–56.
- Lorenz S, Frenzel R, Paschke R, Breitwieser GE, Miedlich SU (2007). Functional desensitization of the extracellular calcium-sensing receptor is regulated via distinct mechanisms: role of G protein-coupled receptor kinases, protein kinase C and beta-arrestins. *Endocrinology* 148, 2398–2404.
- Lowther KM, Uliasz TF, Gotz KR, Nikolaev VO, Mehlmann LM (2013). Regulation of constitutive GPR3 signaling and surface localization by GRK2 and beta-arrestin-2 overexpression in HEK293 Cells. *PLoS One* 8, e65365.
- Luker KE, Steele JM, Mihalko LA, Ray P, Luker GD (2010). Constitutive and chemokine-dependent internalization and recycling of CXCR7 in breast cancer cells to degrade chemokine ligands. *Oncogene* 29, 4599–4610.
- Mackintosh C (2004). Dynamic interactions between 14-3-3 proteins and phosphoproteins regulate diverse cellular processes. *Biochem J* 381, 329–342.
- Marchese A, Paing MM, Temple BR, Trejo J (2008). G protein-coupled receptor sorting to endosomes and lysosomes. *Annu Rev Pharmacol Toxicol* 48, 601–629.
- Maresca M, Mahfoud R, Garmy N, Kotler DP, Fantini J, Clayton F (2003). The virotoxin model of HIV-1 enteropathy: involvement of GPR15/Bob and galactosylceramide in the cytopathic effects induced by HIV-1 gp120 in the HT-29-D4 intestinal cell line. *J Biomed Sci* 10, 156–166.
- Marion S, Weiner DM, Caron MG (2004). RNA editing induces variation in desensitization and trafficking of 5-hydroxytryptamine 2c receptor isoforms. *J Biol Chem* 279, 2945–2954.
- Miller WE, Houtz DA, Nelson CD, Kolattukudy PE, Lefkowitz RJ (2003). G-protein-coupled receptor (GPCR) kinase phosphorylation and beta-arrestin recruitment regulate the constitutive signaling activity of the human cytomegalovirus US28 GPCR. *J Biol Chem* 278, 21663–21671.
- Muro S, Schuchman EH, Muzykantov VR (2006). Lysosomal enzyme delivery by ICAM-1-targeted nanocarriers bypassing glycosylation- and clathrin-dependent endocytosis. *Mol Ther* 13, 135–141.
- Namkung Y, Sibley DR (2004). Protein kinase C mediates phosphorylation, desensitization, and trafficking of the D2 dopamine receptor. *J Biol Chem* 279, 49533–49541.

- Nguyen LP, Pan J, Dinh TT, Hadeiba H, O'Hara E 3rd, Ebtikar A, Hertweck A, Gokmen MR, Lord GM, Jenner RG, et al. (2015). Role and species-specific expression of colon T cell homing receptor GPR15 in colitis. *Nat Immunol* 16, 207–213.
- Okamoto Y, Shikano S (2011). Phosphorylation-dependent C-terminal binding of 14-3-3 proteins promotes cell surface expression of HIV co-receptor GPR15. *J Biol Chem* 286, 7171–7181.
- Padron D, Tall RD, Roth MG (2006). Phospholipase D2 is required for efficient endocytic recycling of transferrin receptors. *Mol Biol Cell* 17, 598–606.
- Paing MM, Johnston CA, Siderovski DP, Trejo J (2006). Clathrin adaptor AP2 regulates thrombin receptor constitutive internalization and endothelial cell resensitization. *Mol Cell Biol* 26, 3231–3242.
- Paing MM, Stutts AB, Kohout TA, Lefkowitz RJ, Trejo J (2002). beta-Arrestins regulate protease-activated receptor-1 desensitization but not internalization or Down-regulation. *J Biol Chem* 277, 1292–1300.
- Pan B, Wang X, Kojima S, Nishioka C, Yokoyama A, Honda G, Xu K, Ikezoe T (2017). The fifth epidermal growth factor like region of thrombomodulin alleviates LPS-induced sepsis through interacting with G-protein coupled receptor 15. *Thromb Haemostasis* 117, 570–579.
- Paradis JS, Ly S, Blondel-Tepaz E, Galan JA, Beautrait A, Scott MG, Enslin H, Marullo S, Roux PP, Bouvier M (2015). Receptor sequestration in response to beta-arrestin-2 phosphorylation by ERK1/2 governs steady-state levels of GPCR cell-surface expression. *Proc Natl Acad Sci USA* 112, E5160–E5168.
- Pearce LR, Komander D, Alessi DR (2010). The nuts and bolts of AGC protein kinases. *Nat Rev Mol Cell Biol* 11, 9–22.
- Pitcher C, Honing S, Fingerhut A, Bowers K, Marsh M (1999). Cluster of differentiation antigen 4 (CD4) endocytosis and adaptor complex binding require activation of the CD4 endocytosis signal by serine phosphorylation. *Mol Biol Cell* 10, 677–691.
- Qian ZM, Li H, Sun H, Ho K (2002). Targeted drug delivery via the transferrin receptor-mediated endocytosis pathway. *Pharmacol Rev* 54, 561–587.
- Rankin ML, Mariniec PS, Cabrera DM, Wang Z, Jose PA, Sibley DR (2006). The D1 dopamine receptor is constitutively phosphorylated by G protein-coupled receptor kinase 4. *Mol Pharmacol* 69, 759–769.
- Ricotta D, Conner SD, Schmid SL, von Figura K, Honing S (2002). Phosphorylation of the AP2 mu subunit by AAK1 mediates high affinity binding to membrane protein sorting signals. *J Cell Biol* 156, 791–795.
- Riddick NE, Wu F, Matsuda K, Whitted S, Ourmanov I, Goldstein S, Goeken RM, Plishka RJ, Buckler-White A, Brenchley JM, Hirsch VM (2015). Simian immunodeficiency virus SIVagm efficiently utilizes non-CCR5 entry pathways in African green monkey lymphocytes: potential role for GPR15 and CXCR6 as viral coreceptors. *J Virol* 90, 2316–2331.
- Rojas R, van Vlijmen T, Mardones GA, Prabhu Y, Rojas AL, Mohammed S, Heck AJ, Raposo G, van der Sluijs P, Bonifacino JS (2008). Regulation of retromer recruitment to endosomes by sequential action of Rab5 and Rab7. *J Cell Biol* 183, 513–526.
- Scarselli M, Donaldson JG (2009). Constitutive internalization of G protein-coupled receptors and G proteins via clathrin-independent endocytosis. *J Biol Chem* 284, 3577–3585.
- Segredo V, Burford NT, Lameh J, Sadee W (1997). A constitutively internalizing and recycling mutant of the mu-opioid receptor. *J Neurochem* 68, 2395–2404.
- Smith AJ, Daut J, Schwappach B (2011). Membrane proteins as 14-3-3 clients in functional regulation and intracellular transport. *Physiology (Bethesda)* 26, 181–191.
- Smyth JW, Zhang SS, Sanchez JM, Lamouille S, Vogan JM, Hesketh GG, Hong T, Tomaselli GF, Shaw RM (2014). A 14-3-3 mode-1 binding motif initiates gap junction internalization during acute cardiac ischemia. *Traffic* 15, 684–699.
- Tobin AB (2008). G-protein-coupled receptor phosphorylation: where, when and by whom. *Br J Pharmacol* 153 (Suppl 1), S167–S176.
- Urs NM, Kowalczyk AP, Radhakrishna H (2008). Different mechanisms regulate lysophosphatidic acid (LPA)-dependent versus phorbol ester-dependent internalization of the LPA1 receptor. *J Biol Chem* 283, 5249–5257.
- van der Sluijs P, Hull M, Webster P, Male P, Goud B, Mellman I (1992). The small GTP-binding protein rab4 controls an early sorting event on the endocytic pathway. *Cell* 70, 729–740.
- Villardaga JP, Jean-Alphonse FG, Gardella TJ (2014). Endosomal generation of cAMP in GPCR signaling. *Nat Chem Biol* 10, 700–706.
- Vitelli R, Santillo M, Lattero D, Chiariello M, Bifulco M, Bruni CB, Bucci C (1997). Role of the small GTPase Rab7 in the late endocytic pathway. *J Biol Chem* 272, 4391–4397.
- Vodros D, Thorstenson R, Doms RW, Fenyo EM, Reeves JD (2003). Evolution of coreceptor use and CD4-independence in envelope clones derived from SIVsm-infected macaques. *Virology* 316, 17–28.
- von Zastrow M, Kobilka BK (1994). Antagonist-dependent and -independent steps in the mechanism of adrenergic receptor internalization. *J Biol Chem* 269, 18448–18452.
- Watari K, Nakaya M, Kurose H (2014). Multiple functions of G protein-coupled receptor kinases. *J Mol Signal* 9, 1.
- Wolfe BL, Trejo J (2007). Clathrin-dependent mechanisms of G protein-coupled receptor endocytosis. *Traffic* 8, 462–470.